

THE THEORY AND APPLICATION OF  
A CONTINUOUS SOURCE IN ATOMIC  
ABSORPTION FLAME SPECTROMETRY

By  
WILLIAM WALTER MCGEE III

A DISSERTATION PRESENTED TO THE GRADUATE COUNCIL OF  
THE UNIVERSITY OF FLORIDA  
IN PARTIAL FULFILLMENT OF THE REQUIREMENTS FOR THE  
DEGREE OF DOCTOR OF PHILOSOPHY

UNIVERSITY OF FLORIDA

December, 1966



## ACKNOWLEDGMENTS

I wish to thank the members of my committee; Dr. L. A. Arnold, Dr. A. P. Black, Dr. W. S. Brey, and Dr. R. C. Stoufer, for their help and advice.

I want to especially thank my research director and committee chairman, Dr. J. D. Winefordner for the help and encouragement he has given me not only in the writing of this dissertation, but throughout my entire stay at the University of Florida.

Also, a very grateful thank you goes to Dr. L. de Galan. Dr. de Galan was the sounding board for many of my ideas. His many suggestions were of invaluable assistance to me.

And finally, my deepest thanks go to my wife, Mary Ann, to whom I dedicate this dissertation. Without her help this study would not have been possible.

## TABLE OF CONTENTS

	Page
ACKNOWLEDGMENTS . . . . .	ii
LIST OF TABLES. . . . .	v
LIST OF FIGURES . . . . .	vi
INTRODUCTION. . . . .	1
EXPERIMENTAL MEASUREMENTS DESIGNED TO ESTABLISH THE RELATIONSHIP BETWEEN THE MEASURED SIGNAL AND THE ATOMIC CONCENTRATION WHEN USING A CONTINUOUS SOURCE OF RADIATION. . . . .	5
Introduction . . . . .	5
Theory . . . . .	6
Atomic absorption measurement with a line source . . . . .	7
Atomic absorption measurement with a continuous source. . . . .	10
A discussion of the curves of growth, total absorption ( $A_T$ ), and the damping constant and present means of calculation . . . . .	14
Experimental Conditions. . . . .	22
Description of the experimental conditions. . .	24
Experimental Results . . . . .	36
Discussion . . . . .	47
Discussion of errors. . . . .	47
Comparison of results with literature data. . .	49
EXPERIMENTAL MEASUREMENTS DESIGNED TO EXTEND ANALYTICAL APPLICATIONS OF THE CONTINUOUS SOURCE .	54
Introduction . . . . .	54

	Page
Experimental . . . . .	55
Apparatus . . . . .	55
Solutions . . . . .	63
Procedure . . . . .	5
Results. . . . .	64
Discussion . . . . .	66
FUTURE WORK. . . . .	74
CONCLUSIONS. . . . .	76
APPENDIX I . . . . .	78
LITERATURE CITED . . . . .	79
BIOGRAPHICAL SKETCH. . . . .	82

## LIST OF TABLES

Table		Page
1.	Specific Components Used in Experimental System for Measurement of the <u>a</u> Parameter. . . .	27
2.	Values of Parameters Dependent Upon Flame Type .	29
3.	Values of Parameters Dependent Upon Element. . .	34
4.	Values of Calculated Spectral and Flame Compositional Parameters . . . . .	44
5.	Values of Spectral and Flame Compositional Parameters Taken from Literature . . . . .	50
6.	Specific Components Used in Experimental System for Measuring Limits of Detection. . . . .	58
7.	Experimental Conditions and Limits of Detection Obtained for 21 Elements Using the Continuous Source. . . . .	61

# LIST OF FIGURES

Figure		Page
1.	Theoretical curves of growth . . . . .	13
2.	Instrumental set-up for the measurement of the <u>a</u> parameter. . . . .	26
3.	Experimental curves of growth for Zn, Cd, and Mg . . . . .	38
4.	Experimental curves of growth for Ag, Cu, and Na . . . . .	40
5.	Illustration of test for location of high density asymptote and <u>a</u> parameter. . . . .	43
6.	Experimental set-up for determining limits of detection with a continuous source . . . . .	57
7.	Analytical absorbance curves for Ag, Cu, and Na obtained using a continuous source. . . . .	68

## INTRODUCTION

Atomic absorption flame spectrometry occupies a unique position among analytical absorption (optical) techniques in that it is the only one which does not use a continuous source of radiation (e.g., tungsten or xenon lamp) for making measurements. Instead, a line source (e.g., hollow-cathode discharge tube or electrodeless discharge tube) emitting very intense radiation over a very narrow range of frequencies is used.

The method of atomic absorption spectrometry was used in astrophysics for investigation of the composition of stellar bodies. Walsh (41), in 1955, indicated that atomic absorption spectrometry should be a useful technique if a flame cell were used to atomize the sample and a line source was used to excite the atomic vapor. However, in his classical paper, Walsh not only surveyed the technique and equipment needed to perform analyses using a line source, but also indicated that a continuous source might have analytical use. He decided that because a monochromator of very high resolution would be needed to resolve the atomic lines under investigation when using a continuous source, a line source of radiation would be easier and much



less expensive to use. In addition, in this paper he presented equations relating the decrease in the peak intensity of the radiation emitted from the line source to the concentration of solution aspirated into the flame. He proved that the measured absorbance when using line sources in atomic absorption analysis was linear with atomic concentration of the sample vapor in the flame gases, and that the technique should be extremely sensitive, that is, limits of detectabilities in the ppm range. Because of these interesting and useful results little work on sources other than line sources was carried out during the next few years. If Walsh had not obtained such excellent results and had not deemphasized the use of a continuous source, atomic absorption analysis might have easily developed along such lines. Astrophysicists such as Ladenburg and Reiche, and van der Held and Ornstein (28,37) in classical experiments measured the amount of energy removed from a continuous source of radiation to determine many classical atom parameters. Expressions for this energy parameter (called total absorption) are well established (28), and in addition to being directly proportional to the absolute atom concentration for dilute atomic gases present in the flame, are independent of the resolving power of the spectrograph.

Developments in atomic absorption analysis using a line source have been numerous and varied. Advances concerning the optical set-up, burner design, flame gases used, and, most important, in analytical applications have tended to make atomic absorption flame spectrometry a more useful analytical technique. Relatively few advances in the line sources have been made, and those that have been made, are aimed at incorporating more than one metal into a line source to enable multi-element analyses to be performed and to increase the intensity of these sources. A few but significant number of developments have occurred in atomic absorption analysis using a continuous source. Gibson, Grossman, and Cooke (16), in 1962, investigated the possibility of using a continuous source for analytical measurements. They concluded that a medium resolution monochromator, when combined with a scale expansion technique, would provide sensitivity comparable with the use of a line source. Recently Ivanov and Kozireva (22), and especially Fassel and co-workers (11,12) have demonstrated that excellent sensitivities are possible when using a continuous source.

With this progress in mind, the aims of this dissertation are then:

(1) To establish the mathematical relationship between atom concentration and measured signal when using a continuous source; verification in the form of working

curves for twelve elements will be given. This working curve is unique, not only in its shape which allows the analyst to detect any deviations from linearity quickly, but in the information concerning fundamental atom parameters which can be obtained from it; such parameters as the a parameter or damping constant (ratio of Doppler and collision half-intensity widths), absolute atom concentration, atom formation efficiency factor, and the total half-intensity width of the line for the atom of concern can be obtained; a discussion of the equipment and procedures used to measure data for preparing the working curves as well as for associated parameters will be given.

(2) To continue the development of the quantitative aspects of atomic absorption using a continuous source; limits of detection for twenty-one elements using an experimental set-up which provides maximum versatility for performing analyses will be given.

# EXPERIMENTAL MEASUREMENTS DESIGNED TO ESTABLISH THE RELATIONSHIP BETWEEN THE MEASURED SIGNAL AND THE ATOMIC CONCENTRATION WHEN USING A CONTINUOUS SOURCE OF RADIATION

## Introduction

When performing quantitative atomic absorption measurements using a line source of radiation, the working curve prepared is usually a plot of absorbance versus solution concentration. If a line source with a half-intensity width less than the absorption line half-width is used, the signal measured corresponds to variation in the maximum absorption coefficient at the central wavelength of interest. Because absorbance is proportional to the atomic absorption coefficient, the working curve is linear only as long as the absorption coefficient is proportional to solution concentration.

When a continuous source of radiation is used, the wavelength interval of continuous radiation isolated by the monochromator depends upon the resolving power of the monochromator. For the case of the medium resolution monochromator used in this study, the spectral band width will be much larger than the line width of the absorbing atoms in the flame. Therefore, the measured absorption signal

will correspond to a function of the absorption coefficient integrated over the spectral band width of the monochromator and will always be proportional to concentration.

As seen from this brief comparison, certain basic differences exist between the absorption signal measured using a line source and a continuous source. Because of these differences, this investigation was carried out to determine if a more accurate and useful relationship (than absorbance) existed between solution concentration and measured signal when using a continuous source of radiation.

### Theory

In order to indicate the similarities and the differences in the use of a continuous source and a line source in atomic absorption spectrometry, it is assumed that the basic equipment consisting of a flame cell, a monochromator, and an electrometer-read-out system are used in both cases. Consequently, the instrumental proportionality factor  $Z$ , relating read-out voltage to intensity of radiation reaching the entrance slit of the monochromator, will be the same in both cases.

All comparisons are made with respect to the type of monochromator used in this study: a medium resolution monochromator capable of isolating a single line, but not capable of resolving the spectral line profile. This means

that the spectral band width of the monochromator  $s$ , is considerably larger than the absorption line half-width  $\Delta\lambda_T$ . In turn, the absorption line half-width is assumed to be larger than the half-width of the line emitted by the line source,  $\Delta\lambda_N$ .

#### Atomic absorption measurement with a line source

The photodetector signal due to radiation emitted by the line source passing through the flame gases with only blank solution being aspirated is given by

$$I_\ell^\circ = \int_{\Delta\lambda_N} J_\lambda^\circ d\lambda, \quad (1)$$

where  $J_\lambda$  is the intensity per unit of wavelength. The signal from the radiation passing through the flame with sample solution being aspirated is given by

$$I_\ell = \int_{\Delta\lambda_N} J_\lambda^\circ e^{-k_\lambda L} d\lambda, \quad (2)$$

where  $L$  is the path length in the flame.

In general, the atomic absorption coefficient  $k_\lambda$ , is a complex function of wavelength and is described by the following set of formulas (30):

$$k_{\lambda} = k_0 \delta(a, v) \quad (3)$$

$$k_0 = \frac{2\sqrt{\pi \ln 2} e^2 \lambda_0^2 N f}{m c^2 \Delta \lambda_D} \quad (4)$$

$$\Delta \lambda_D = \frac{\lambda_0}{c} \sqrt{\frac{8RT \ln 2}{M}} \quad (5)$$

$$\delta(a, v) = \frac{a}{\pi} \int_{-\infty}^{+\infty} \frac{e^{-y^2} dy}{a^2 + (v-y)^2} \quad (6)$$

where  $e$  and  $m$  are the charge and mass of the electron,

$c$  is the velocity of light,

$\lambda_0$  is the wavelength at the line center,

$f$  is the oscillator strength,

$N$  is the concentration of absorbing atoms in the flame,

$T$  is the flame temperature,

$R$  is the gas constant,

$M$  is the atomic mass,

$\Delta \lambda_D$  is the Doppler half-intensity width of the absorption line,

$a$  is the damping constant, given approximately by  $\frac{\Delta \lambda_L \sqrt{\ln 2}}{\Delta \lambda_D}$ ,

$\Delta \lambda_L$  is the collision (Lorentz) half-width of the absorption line,

and  $v$  is equal to  $\frac{2\sqrt{\ln 2} (\lambda - \lambda_0)}{\Delta \lambda_D}$ .

The function  $S(a, \nu)$  describes the variation of  $k_\lambda$  over the source line line. However, the integration in equation 2 extends over the emission line width,  $\Delta\lambda_N$ , only, which is generally much smaller than the absorption line width. If we replace  $k_\lambda$  with

$$\bar{k} = k_0 S(a, \bar{\nu}), \quad (7)$$

where  $\bar{k}$  represents the average absorption coefficient over the source line width  $\Delta\lambda_N$ , and  $\bar{\nu}$  is an average over the range from zero to  $\Delta\lambda_N$ , then the absorbance is given by

$$A_p = \ln \frac{I_0}{I_p} = \bar{k} L, \quad (8)$$

or, for small concentrations, when  $\bar{k}L \ll 1$ ,

then

$$A_p = \bar{k}L = k_0 S(a, \bar{\nu})L = \frac{2\sqrt{2\pi} \ln 2^2 \lambda_0^2 HFL S(a, \bar{\nu})}{m c^2 \Delta \lambda_D}. \quad (9)$$

It follows from equations 8 and 9 that if a line source is used in atomic absorption spectrometry, such a plot should produce a straight line as long as the atom concentration in the flame is proportional to its concentration in solution. When a very narrow line source is used (i.e.,  $\Delta\lambda_N \ll \Delta\lambda_D$ ,  $\bar{\nu} \approx 0$ ), this straight line should extend over an extremely large concentration range; namely, up to the point where resonance broadening causes the damping constant to change (30) (for molar solution concentrations).



Normally, linearity over an extended range of concentration is not found. Deviations can be attributed to:

(1) Ionization and compound formation of the atom of concern.

(2) A nonlinear relationship between atom concentration in the flame (N), and solution concentration (C).

(3) Variations in aspiration efficiency (43).

(4) The source line width is no longer negligible when compared to the absorption line width.

Rubeska and Svoboda (34), and Vickers, Remington and Winefordner (40) have discussed other sources of deviations found in atomic absorption flame spectrometry.

#### Atomic absorption measurement with a continuous source

With a line source, the wavelength region of interest is determined by the width of the source line; whereas, for the case of a continuous source, this region is determined by the spectral band width of the monochromator,  $s$ . Over this small range of frequencies the intensity of the source is essentially constant; therefore, the blank photodetector signal is given by

$$I = z \int J_{\lambda}^{\circ} = J_{\lambda_0}^{\circ} s. \quad (10)$$

The photodetector signal due to radiation passing through the flame with sample solution being aspirated is then

$$I_c = \int J_{\lambda}^{\circ} e^{-k_{\lambda} L} d\lambda = \int J_{\lambda_0}^{\circ} \int e^{-k_{\lambda} L} d\lambda, \quad (11)$$

therefore, the fraction of intensity absorbed in the flame is given by

$$\alpha_c = \frac{I_c^{\circ} - I_c}{I_c^{\circ}} = \frac{\int_0^{\infty} (1 - e^{-k_{\lambda} L}) d\lambda}{S} = \frac{A_T}{S}, \quad (12)$$

where the integration limits are 0 to  $\infty$  because the spectral band width is assumed to be much larger than the width of the absorption line and where  $A_T$  is known as the total absorption (28,30,36). Curves representing  $A_T$  as a function of the concentration  $N$ , depend on the value of the damping constant  $a$ , and are referred to as curves of growth (21,28,30,38).  $A_T$ ,  $a$ , and curves of growth will be discussed in the next section. An important characteristic of  $A_T$  which can be seen from the curve of growth is,  $A_T$ , is proportional to  $N$  at low concentrations and proportional to  $N^{1/2}$  at very high concentrations. Where  $k_{\lambda} \ll 1$  for the low concentration region, when Doppler broadening is assumed predominant, equation 12 becomes

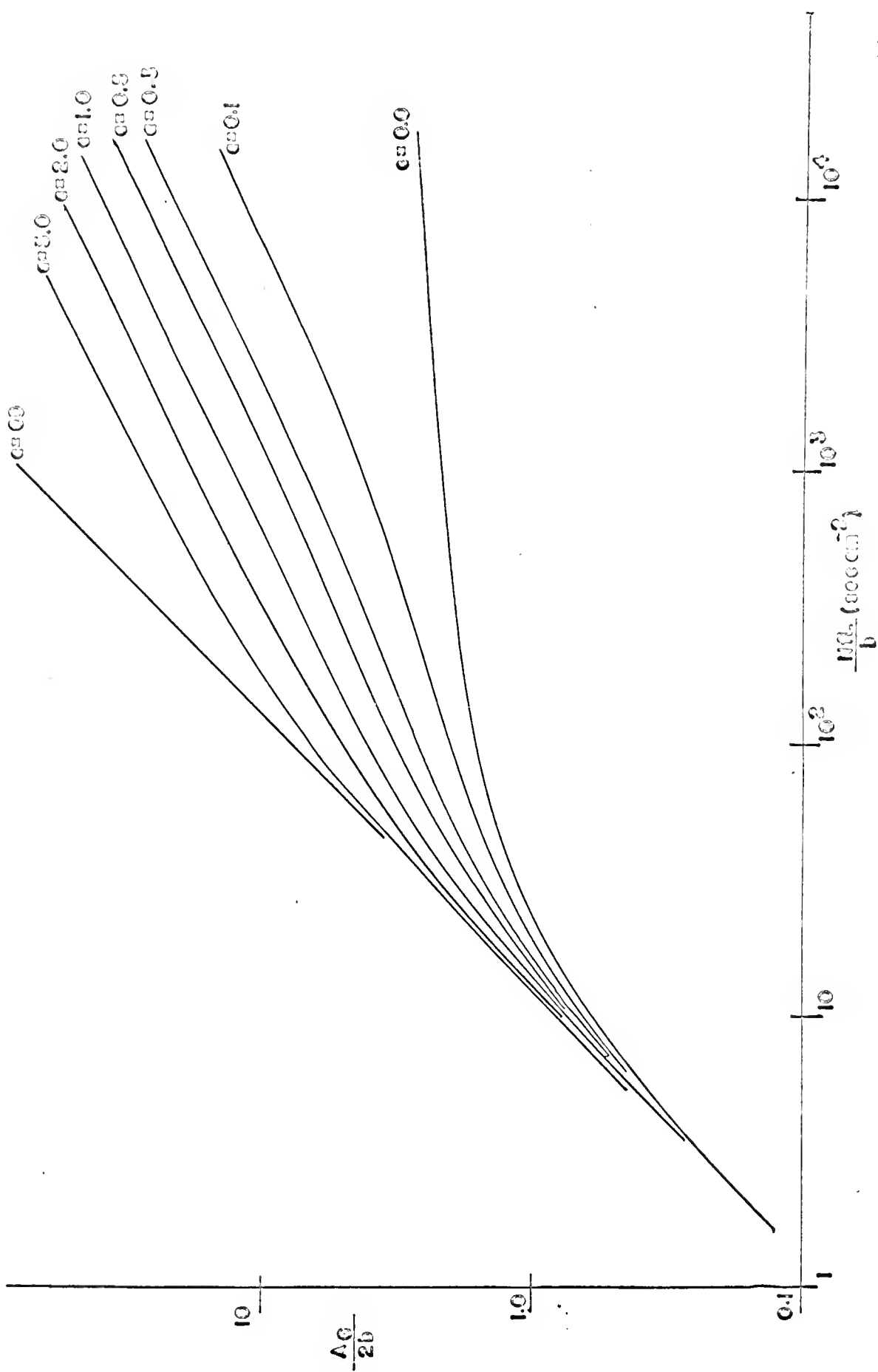
$$\alpha_c = \frac{\int_0^{\infty} k_{\lambda} L d\lambda}{S} = \frac{k_0 L \sqrt{\pi} \Delta\lambda_D}{2 \sqrt{\ln 2} S} = \frac{\pi L^2 \lambda_0^2 N f L}{m c^2 S}, \quad (13)$$

which is independent of the absorption line profile. This can be seen from the similarity of all the curves of growth (see Figure 1) for the low concentration region. The

Fig. 1.--Theoretical curves of growth (38).

For a single spectral line for various  $\underline{a}$

$$\text{parameter values. } b = \frac{\pi \Delta D}{(n 2)^{1/2}} ; A_G = A_T.$$



general expression for the absorbance A, is then

$$A_c = \ln \left( \frac{I_c^0}{I_c} \right) = -\ln \left( 1 - \frac{A_T}{S} \right) \quad (14)$$

As can be seen from this relationship, absorbance is a complicated function of the concentration of the element in the flame. According to equation 14, the absorbance is proportional to the total absorption  $A_T$ , only for small values of the ratio  $\frac{A_T}{S}$ . On the other hand, the fraction of intensity absorbed in the flame  $\alpha_c$ , is always proportional to the total absorption, but will be linear only over the linear portion of the curve of growth. De Galan (7) has shown that both types of working curves (absorbance or relative absorption versus concentration), when prepared from measurements made with a continuous source, begin to slope off when more than 10 per cent of the radiation is absorbed in the flame. At lower values of relative absorption, linear expansion of  $A_T$  in equation 14 is valid. Therefore, both types of working curves will show a similar linear range over the low concentration range.

A discussion of the curves of growth, total absorption ( $A_T$ ), and the damping constant and present means of calculation

To establish the validity and to provide a better understanding of these parameters, a discussion of the

general nature and present means of calculation is presented in this section. The discussion of the value and use of these parameters in this study will be presented in a later section.

Total absorption ( $A_T$ ), as defined by Ladenburg and Reiche (28), is the fraction of energy removed over the wavelength interval of the spectral line from a continuous spectrum by atoms in an absorbing column of gas. It is given mathematically by the expression

$$A_T = \int_0^{\infty} (1 - e^{-K_{\lambda} L}) d\lambda. \quad (15)$$

Minkowski (29), in a series of experiments, showed this parameter to be independent of the slit width of the monochromator within the limits of experimental error.

The curve of  $A_T$  plotted against the absolute number of absorbing atoms is called a theoretical curve of growth. Classically, this plot was used in experiments to determine many fundamental parameters concerning the atom; some examples are the number of dispersion electrons associated with the emission and absorption of a particular line, and the natural lifetime of an atom. As seen from the theoretical curves of growth in Figure 1, each curve is characterized by a linear range where  $A_T$  is proportional to  $N$  in the low concentration region; the curve gradually slopes off in the high concentration range to become proportional to  $N^{1/2}$ .

While each curve is characterized by slopes of 1 and 1/2, exact position of each curve is dependent upon the damping constant or a parameter. This constant was previously defined in equation 6 as

$$a = \frac{\Delta \nu_L \sqrt{\ln 2}}{\Delta \nu_D}^* \quad (6a)$$

Until recently, theoretical curves of growth were available for only a few scattered a parameters (33). Recently van Trigt, Hollander, and Alkemade (38) provided useful calculations for preparing theoretical curves of growth for a parameter values ranging from 0 to 10, with the values from 0 to 1 given in 0.1 units. The latter range will be of great use to flame spectroscopists because of conditions found in the flame.

Interest in the a parameter stemmed from the fundamental data which can be calculated from it. Information concerning the interaction of perturbing and emitting particles (i.e., the optical cross-section), the resultant wavelength distribution of emitted intensity (i.e., the line profile), and in combination with a curve of growth, the absolute atom concentrations, and efficiency of atom formation in (e.g.) flames, are just a few of the more

---

\* From now on, all formulas will be given in terms of frequency units. Those formulas previously calculated in terms of wavelength units can be converted by the following expressions:  $\nu = c/\lambda$  and  $\Delta \nu = (c/\lambda^2) \Delta \lambda$ .

important parameters which can be calculated. Experimentally, a is a difficult parameter to determine; therefore, most measurements are made on the emission intensity from flames of low burning velocity (e.g., acetylene-air). In general, few a parameters have been measured (even in these flames) because of the restrictions placed on the types of flames and flame conditions which can be used to prepare curves of growth in emission from which they are determined. The requirements for the preparation of the curves of growth in emission are (21):

(1) A homogeneous distribution of flame gas and metal species.

(2) A homogeneous distribution of temperature over the region of observation.

(3) Complete elimination of self-reversal.

(4) Complete elimination of ionization.

(5) Linearity of aspiration and photodetector-amplifier read-out.

For these reasons, no measurements have been made in flames of high burning velocity (e.g., acetylene-oxygen and hydrogen-oxygen) which are of use in analytical flame spectrometry.

Two methods based on measurement of the variation of intensity of radiation emitted by atoms in the flame for preparing curves of growth are available for accurate determination of the a parameter. The newest method developed



by van Trigt, Hollander, and Alkemade (38) utilizes experimental and theoretical curves of growth in combination with an experimental duplication curve to determine the a parameter and absolute atom concentration directly. The reader's attention is called to this article for a more detailed discussion of the method used.

The older and more widely known method is the one developed by Hinnoy and Kohn (18,19). In their classical papers, the authors presented equations for the high and low density asymptotes of the curve of growth which take into account their dependence on the a parameter. They showed that the absolute ordinate of the point of intersection of the asymptotes (see Figures 3 and 4) is

$$\log \frac{A_T \sqrt{\ln 2}}{\Delta \nu_D} = \log 2a^* \quad (16)$$

Thus from a knowledge of the temperature of the flame and a series of experimentally measured  $A_T$  values, the a parameter could immediately be determined. The  $A_T$  values necessary to prepare the experimental curve of growth were determined from the measured variation of intensity from atoms in a series of metal solutions aspirated into a flame of low

---

\*In more recent papers by Behmenburg and Kohn (1,2), the effects of hyperfine structure due to nuclear spin and isotopic shift on the value of the ordinate were studied. They found the ordinate value equal to  $\log na$ , where  $n$  is a constant, the value of which is dependent upon the atom under consideration.

burning velocity. The measured emission intensity was converted to total intensity (absorption) by comparison with the radiation from a standard lamp.

The curve of growth prepared in this manner is an experimental curve of growth because the abscissa of this plot is solution concentration. The intersection point of the high and low density asymptotes is also necessary for converting experimental solution concentration to absolute atom concentration in the flame gases.

The relationship\*

$$K = \frac{4a}{\pi C_I} \quad , \quad (17)$$

allowed calculation of the proportionality constant K which related the theoretical and experimental curves of growth to  $C_I$ , which is the solution concentration at the intersection point. Therefore, at any solution concentration C, the concentration of atoms in the flame capable of absorbing the line under consideration was given by

$$N_j = \frac{mc \Delta \nu_0 K C}{2 e^2 f L \gamma \ln 2} \quad . \quad (18)$$

This value of  $N_j$  represents the population in energy level j, and can be converted to the total number of free atoms of

---

\*The proportionality constant K is labeled Q in Hinnoy and Kohn's (18,19) work.

the element by using the Boltzmann distribution relationship.

Once the  $\underline{a}$  parameter and absolute atom concentration have been determined, many other parameters of interest can be calculated.

The efficiency of atom formation  $\beta_I$ , at the intersection point is calculated from the following relationship:

$$\beta_I = \frac{N_I}{N_{\text{total}}} = \frac{N_I}{3 \times 10^{21} \left( \frac{n_{298}}{n_T} \right) \left( \frac{C_I \bar{F} \epsilon}{QT} \right)}, \quad (19)$$

where  $N_I$ , is the absolute atom concentration at the intersection point;

$N_{\text{total}}$ , is the total number of atoms present regardless of form;

$\bar{F}$ , is the solution flow rate in cc./min.;

$n_{298}$  and  $n_T$ , are the total number of moles of flame gas products present at 298° K and at the flame temperature T;

$Q$ , is the flow rate of unburned gases in cc./min.;

and

$\epsilon$ , is the aspiration efficiency as defined by Winefordner, Mansfield, and Vickers (43).

As defined,  $\beta_I$ , is a factor used to account for atomic losses due to ionization and dissociation of the salt

introduced and compounds formed between the atomic species of interest and various gas products.

The collision (Lorentz) half-intensity width  $\Delta\nu_L$  (30,36) is given by

$$\Delta\nu_L = \frac{a \Delta\nu_0}{\sqrt{\ln 2}} \quad , \quad (20)$$

and the total half-intensity width of the line  $\Delta\nu_T$  (30,36) is given by

$$\Delta\nu_T = \sqrt{(\Delta\nu_L)^2 + (\Delta\nu_0)^2} \quad . \quad (21)$$

Normally, natural broadening and resonance broadening will not be significant when compared to Doppler and collisional broadening. Natural broadening is on the order of  $10^{-4}$  Å, resonance broadening does not become appreciable until molar solutions are used, Doppler and collisional broadening are on the order of  $10^{-1}$  -  $10^{-2}$  Å. For this reason natural and resonance broadening will not be considered in this paper.

The effective cross-section for collision (Lorentz) broadening (30,36)  $\sigma_L$ , is given by

$$\sigma_L^2 = \frac{\Delta\nu_L}{1.36 \times 10^{25} P_f \left[ \frac{1}{T} \left( \frac{1}{M} + \frac{1}{M_a} \right) \right]^{\frac{1}{2}}} \quad , \quad (22)$$

where  $P_f$ , is the pressure on the system during measurement (normally taken to be 760 mm);

$M$ , is the atomic weight of the absorbing species; and  $M_a$ , is an effective molecular weight of the flame gas species including water which causes collisional broadening.

This parameter ( $\sigma_L$ ) is of interest because it can be used to indicate the nature and type of interaction between perturbing and emitting species.

### Experimental Conditions

As can be seen from the theory developed for the signal measured using a continuous source, the absorption method can be used to determine total absorption ( $A_T$ ) directly.\* A valid test of the relationship would be to prepare working curves (experimental curves of growth), to check for correct shape (i.e., the correct slopes), and to calculate reasonable a parameters. The method could then be used to calculate other parameters such as atom formation efficiency, total line width, and effective collisional cross section; however, these values could not be used as conclusive proof of the method because they represent the first to be calculated in this type of flame.

The preparation of the curves of growth from absorption measurements also offered other advantages which

---

\*  $A_T/s$  is obtained from the experimental curve and is converted to  $A_T$  by multiplying by the spectral band width  $s$ .

overcome some of the restrictions inherent in the emission method. Some of these advantages are:

(1) Self-reversal will not influence the value of a measured absorption signal.

(2) For those atoms which do not form compounds or ionize readily, small variations in temperature will have little effect on absolute atom concentration (8).

(3) Atoms which emit radiation too weak to be detected reliably can still be measured using an absorption technique.

(4) The absolute number of atoms producing the absorption is obtained directly. Generally the total number of atoms producing absorption is approximately the same as the total number of atoms in all states. However, if this situation is not valid, then the atomic concentration calculated from equation 18 can be converted to the total number of atoms in all states by use of the Boltzmann equation. An example of this case is Ni ( $3414 \text{ \AA}$ ) where the absorption transition originates from a low lying energy level.

In this study, curves of growth will be prepared for twelve elements from measurements of the variation of the fraction of intensity absorbed with concentration of aspirated solution using a total-consumption aspirator burner for five flames of interest in analytical flame spectrometry.

The choice of hydrogen and acetylene as a fuel and oxygen as the oxidant, and their respective flow rates to

produce stoichiometric or fuel-rich flames was determined by their relative usefulness for analytical flame spectrometry. The argon-hydrogen-entrained air (Ar/H<sub>2</sub>-E.A.) flame was added to this list because of recent successes with this flame in this laboratory (39,46).

With respect to the requirements for preparing curves of growth in emission (referred to earlier), those not covered by the inherent advantages of the absorption method will be met by:

(1) Reducing ionization by addition of an ionization buffer to solutions of those metals with ionization potentials below 5 e.v.

(2) Reducing the variation of temperature and composition in the flame region viewed by judicious choice of the location and size of the flame region viewed.

The a parameters and absolute atom concentrations will be calculated from the curve of growth by the method developed by Hinnov and Kohn (18,19).

#### Description of the experimental conditions

(a) Conditions for measurement of the a parameter.

The instrumental set-up used for making the flame absorption measurements is shown in schematic form in Figure 2. The specific components used in the experimental set-up are given in Table 1, and the operating conditions for the measurements are given in Table 2.

Fig. 2.-Instrumental set-up for the measurement of the a parameter.



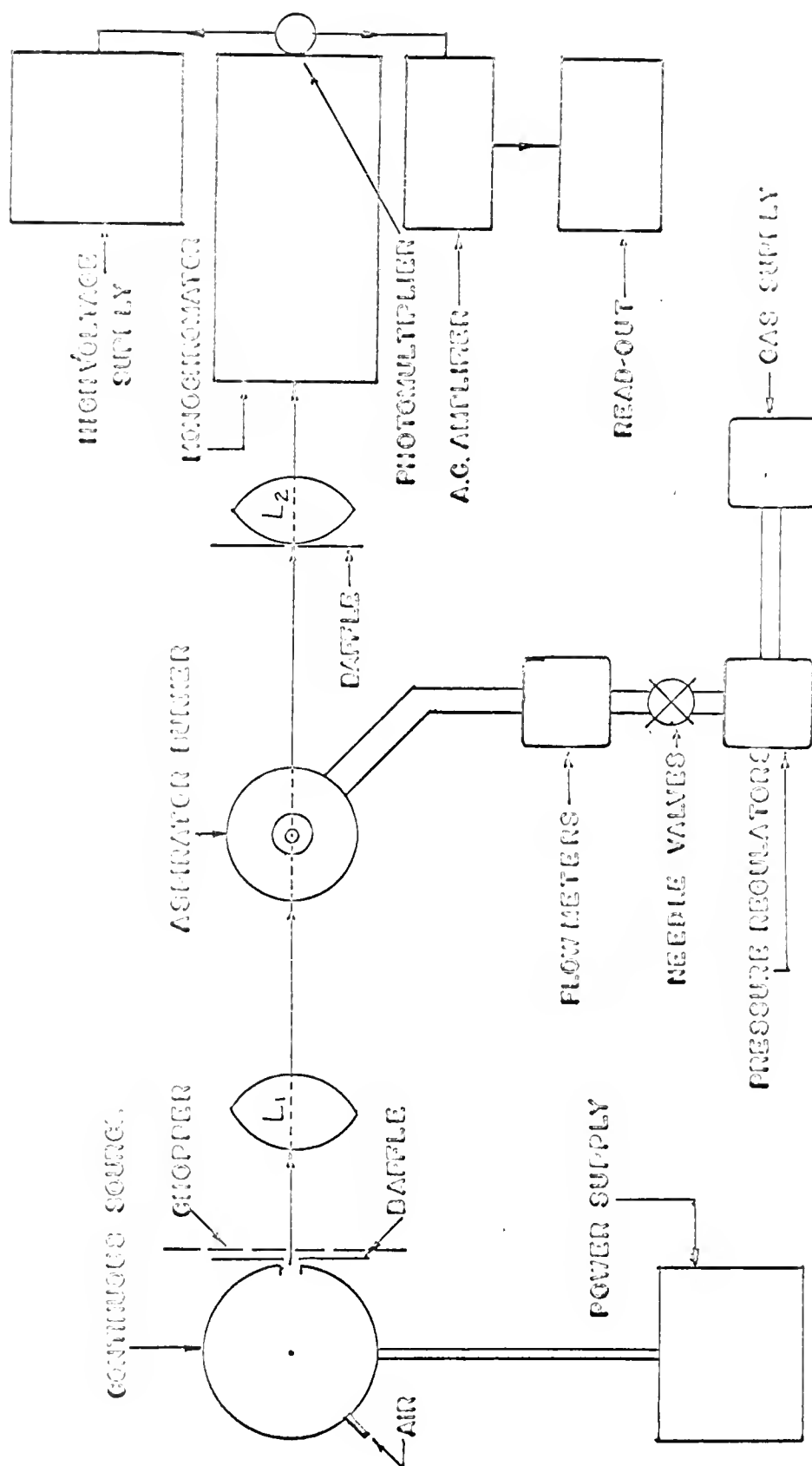


TABLE 1

SPECIFIC COMPONENTS USED IN EXPERIMENTAL SYSTEM FOR  
MEASUREMENT OF THE  $a$  PARAMETER

1. Spectral Continuum      Xenon arc, 150-watt (Englehard, Hanovia, Newark, N. J.) powered by a regulated a.c. supply (Sola Electric Co., Chicago, Ill.).
2. Optics      Single pass, chopped at 320 cps. Chopper consists of a disc with eleven equally spaced holes rotated by an 1800 rpm synchronous motor (Bodine Electric Co., Chicago, Ill.).  $L_1$  and  $L_2$  are quartz lenses.
3. Monochromator      Jarrell-Ash, Model 82000, 0.5 meter Ebert Mount, grating spectrometer (Jarrell-Ash Co., Waltham, Mass.). Grating is ruled for 1250 lines/mm. and is blazed at 5000 Å (for Zn, Cd, and Mg a 3000 Å blazed grating was used).
4. Detector-Power Supply      EMI 9558 QB photomultiplier (1650-9000 Å). Regulated d.c. power supply (No. 418A, Fluke Mfg. Co., Seattle, Wash.).
5. Amplifier-Readout Electronics      A.C. Photomultiplier output signal was fed into an O.R.N.L. No. 7 a.c. amplifier turned to 320 cps. The plate and filament voltages were taken from a dual power supply (No. R 100 B, Philbrick Researches, Boston, Mass.). The a.c. signal was rectified and the d.c. signal was recorded on a potentiometric recorder (Model TR, E. H. Sargent and Co., Chicago, Ill.). A scale expansion technique was used where necessary.

6. Gas Pressure and Flow  
Regulation

The gas flow is regulated by a Beckman High Precision regulation unit (No. 9220, Beckman Industries, Fullerton, Calif.). The resultant flow is monitored by rotammeters (No. 4-15-2 Ace Glass Co., Inc., Vineland, N. J.).

7. Aspirator-Burner

Total-Consumption Type (Carl Zeiss Inc., New York, N. Y.).

TABLE 2

VALUES OF PARAMETERS DEPENDENT UPON FLAME TYPE

Gas Type	Flow Rate (l/min.)		Height <sup>c</sup>	T°K <sup>d</sup>	$\epsilon$	$\bar{\phi}$ (cc./min.)	L (cm.)	Ma (g./m.)	Q (cc./sec.)
	Fuel	Oxidant							
H <sub>2</sub> /O <sub>2</sub> ST. <sup>a</sup>	10.0 - H <sub>2</sub>	5.0 - O <sub>2</sub>	1.25 in.	2535	0.82	2.5	2.5	16.5	246
H <sub>2</sub> /O <sub>2</sub> F.R. <sup>b</sup>	12.0 - H <sub>2</sub>	5.0 - O <sub>2</sub>	1.45 in.	2560	0.87	2.5	2.5	10.9	283
Ar/H <sub>2</sub> E.A.	8.5 - H <sub>2</sub>	3.0 - Ar	1.45 in.	1860	0.75	5.0	2.7	26.3	192
C <sub>2</sub> H <sub>2</sub> /O <sub>2</sub> ST.	2.0 - C <sub>2</sub> H <sub>2</sub>	5.0 - O <sub>2</sub>	0.75 in.	2625	0.89	2.5	1.0	27.3	118
C <sub>2</sub> H <sub>2</sub> /O <sub>2</sub> F.R.	3.25 - C <sub>2</sub> H <sub>2</sub>	5.0 - O <sub>2</sub>	1.25 in.	2730	0.95	2.5	2.4	25.2	137

<sup>a</sup>ST. = stoichiometric fuel - oxidant mixture.<sup>b</sup>F.R. = fuel rich fuel - oxidant mixture.<sup>c</sup>Height viewed in flame was taken with respect to burner tip.<sup>d</sup>Error in flame temperature is  $\pm 50^\circ\text{K}$ .

Stock solutions of 20,000 ppm for each of the twelve elements were prepared by dissolving the appropriate salt (chloride or nitrate) in aqueous or the metal in acidified-aqueous solution. More dilute solutions were made by successive dilution of the stock solution. The ionization buffer salt ( $\text{CsNO}_3$  or  $\text{KNO}_3$ ) was added to each dilution of the stock solution for the alkali metals in quantities as prescribed by Hoffman and Kohn (20) (i.e.,  $2 \times 10^{-3} \text{ M}$   $\text{K}_2\text{CO}_3$  for Li and Na,  $2.5 \times 10^{-1} \text{ M}$   $\text{K}_2\text{CO}_3$  for Rb, and  $1 \times 10^{-1} \text{ M}$   $\text{CsNO}_3$  for K).

The flow rates for the gases used to produce the flames used in this study are given in Table 2. The region of the flame chosen for investigation in the total-consumption aspirator burner was, in all cases, located a short distance above the inner cone in the interconal region of the flame (see Table 2 for respective heights). This region was chosen to insure that equilibrium statistics controlled the concentration of the species present in this region (17).

The entrance optics and slit height of the experimental set-up were used to control the size of the region viewed and to reduce it to a minimum according to the restrictions discussed by Hollander (21).

The temperature of the interconal region of the flame was measured by the line-reversal method for the Ar/ $\text{H}_2$ -E.A. and  $\text{H}_2/\text{O}_2$  flames. The line-reversal method of Féry (13) as

discussed by Gaydon and Wolfhard (15), is based on the assumption that, on introducing metal atoms in the flame, statistical equilibrium is established between the electronic degrees of freedom of the metal atoms and flame gases. The metal atoms thus emit and absorb their spectral lines as thermal radiators. The line-reversal method is based on the following principle: If a blackbody is placed behind a flame containing sodium atoms which are emitting the yellow sodium D doublet, and a spectrometer is aligned to see both the blackbody and flame simultaneously, then there will be some temperature of the blackbody at which its brightness for the specific wavelength region equals the brightness of the blackbody transmitted through the flame, plus the brightness of the D lines from the flame. At this temperature, only a continuous spectrum of the blackbody will be recorded. At a lower temperature of the blackbody, the sodium line will appear in emission superimposed upon the continuous background; and at a higher temperature, the sodium line will appear in absorption. The brightness temperature of the standard tungsten lamp was calculated as a function of lamp current from data for the radiance at 35 amperes supplied as a calibration with the lamp and the emissivity of tungsten at  $5890 \text{ \AA}$  calculated by de Vos (10).

The two-line method was used for the hotter  $\text{C}_2\text{H}_2/\text{O}_2$  flames and also for the  $\text{H}_2/\text{O}_2$  flames in order to compare the results of the two methods.

The Ornstein two-line method (3) involved the measurement of the intensities of two iron lines; Fe 3734.87 Å, and Fe 3737.14 Å, from which the temperatures can be calculated by the following formula:

$$\log \frac{I_a}{I_b} = \log \frac{A_{g_a}}{A_{g_b}} + \log \frac{\lambda_b}{\lambda_a} + \frac{E_b - E_a}{kT} \quad , \quad (22)$$

where  $I_a$  and  $I_b$  are the relative measured intensities at  $\lambda_a = 3734.87 \text{ Å}$  and  $\lambda_b = 3737.14 \text{ Å}$  lines, respectively;  $A_{g_a}$  and  $A_{g_b}$  represent the product of the transition probability and statistical weight for the two lines (the ratio of  $A_{g_a}$  to  $A_{g_b}$  was calculated from data given by Crosswhite (6) and found to be equal to 11.6);  $E_a$  and  $E_b$  are the energy of the transition corresponding to the line;  $k$  is the Boltzmann constant; and  $T$  is the flame temperature of interest.

Crosswhite (6), and Broida and Lalos (4), have discussed some of the requirements for use of this method. A few more of the more important requirements are:

- (1) Both lines chosen must have negligible self-absorption and self-reversal or at least have them of equal degree.
- (2) Lines must be close enough for rapid but accurate scanning.
- (3) Both lines must be close enough together to insure that the photocathode has essentially the same

response to both lines or a suitable correction must be made. The agreement of the temperatures obtained by the two methods was excellent and within experimental error. The experimental set-up used for the temperature measurements was the same as shown in Figure 2, except that the continuous source was replaced by a standard tungsten lamp. The temperatures determined for these regions are given in Table 2.

The spectral band width of the monochromator (see Table 3) was determined by scanning the  $3650.15 - 3654.83 \text{ \AA}$ , and  $5769.59 - 5790.65 \text{ \AA}$  lines from a low pressure Hg discharge lamp. The relative recorded distance between the two lines was converted to a known distance, and this scale was used to measure the half-intensity widths of the lines involved. The relative standard deviation in measuring the spectral band width was less than 10 per cent for all slit widths used. This method is preferred to the scanning of a single line (e.g., the iron lines used in the temperature measurements) because of the difficulty encountered in reproducing the exact scanning speed. The experimental set-up used for this measurement was the same as that shown in Figure 2, except the total-consumption aspirator-burner was replaced by the Hg lamp.

Because metal concentrations ranged from  $1 - 10^4$  ppm, the output of the detector-amplifier system was checked for linearity of response by use of neutral density filters of



TABLE 3  
VALUES OF PARAMETERS DEPENDENT UPON ELEMENT

Element	$\lambda_0$ (Å)	$f$	Site Width (Å)	Spectral Band Width (Å)
Li	6707	0.75	80	0.90
Na	5890	0.67	210	3.14
K	7665	0.67	300	3.66
Rb	7800	0.67	200	2.92
Cu	3247	0.30	12	0.38
Ag	3281	0.51	12	0.38
Mg	2852	1.11	40	0.41
Ca	4227	1.55	12	0.38
Sr	4607	1.80	12	0.38
Ni	3414	0.11	12	0.38
Zn	2138	1.30	40	0.41
Cd	2288	1.25	40	0.41

known transmission and found to be satisfactory. The relative error due to deviations from linearity of aspiration was also checked and found to be less than 3 per cent for all solutions with metal concentration less than  $2.5 \times 10^{-4}$  ppm.

b. Conditions for measurement of the atom efficiency factor,  $\beta_I$ .

The aspiration efficiency ( $\epsilon$ ), is a measure of the ability of the flame to remove the solvent from the salt solution aspirated into the flame (31,43). As such, it is a difficult quantity to measure because of its strong dependence upon height in the flame and flame gas composition. Parsons and Winefordner (31) have suggested a method of measuring  $\epsilon$ , based on a comparison of the measurements of the light reflected from water droplets aspirated from the burner, with and without the flame. Using their method, the aspiration efficiencies for the five flames under investigation for the specific region of interest were measured (see Table 2).

The value of the path length of radiation through the flame ( $L$ ) for a total consumption burner (see Table 2) is difficult to measure due to the irregular shape of the turbulent flame. The value of  $L$  can be approximated by measuring the length of the path over which continuum radiation is scattered when solution is aspirated into the burner (flame not burning).

The solution flow rate  $\bar{\phi}$ , was determined from the time required for aspiration of a known volume of salt solution (see Table 2). The standard deviation in all cases was less than 1 per cent.

The value of  $Q$ , the flow rate of unburned gases, can be calculated from a simple conversion of the flow rates of gases used to produce the flame (see Table 2).

The value of the parameter  $n_{298}/n_T$  which corrects for the expansion of the total number of moles of flame gases for the temperatures indicated was calculated and found to be equal to the value determined by Winefordner and Vickers (44,45). The value of this ratio is 0.83.

### Experimental Results

Curves of growth were prepared from absorption measurements for each element in each of the five flames. Each point on the curve represented the average value of nine determinations with a relative standard deviation of less than 1 per cent. Examples of several curves are given in Figures 3 and 4, for Zn in  $C_2H_2/O_2$  (stoichiometric), cadmium in  $H_2/O_2$  (fuel-rich), and Mg, Na, Cu, and Ag in Ar/ $H_2$ -E.A. From the value of the total absorption  $A_T$ , taken from the intersection point of the asymptotes of a specific experimental curve of growth and the Doppler half-intensity width calculated from flame temperatures, the a parameter

Fig. 3.-Experimental curves of growth for Zn, Cd, and Mg.

One - Zinc, 2138 Å line, in C<sub>2</sub>H<sub>2</sub>/O<sub>2</sub> ST.

Two - Cadmium, 2288 Å line, in H<sub>2</sub>/O<sub>2</sub> F.R.

Three - Magnesium, 2852 Å line, in Ar/H<sub>2</sub>-E.A.

(In experimental and theoretical coordinates.

Note, the right ordinate is  $A_T \sqrt{\ln 2} / \Delta \nu_D$

where  $A_T$  and  $\Delta \nu_D$  are in units of sec<sup>-1</sup>.

However, the same ordinate values would

result if  $A_T \sqrt{\ln 2} / \Delta \lambda_D$  were plotted, where

$A_T$  and  $\Delta \lambda_D$  are in wavelength units.)

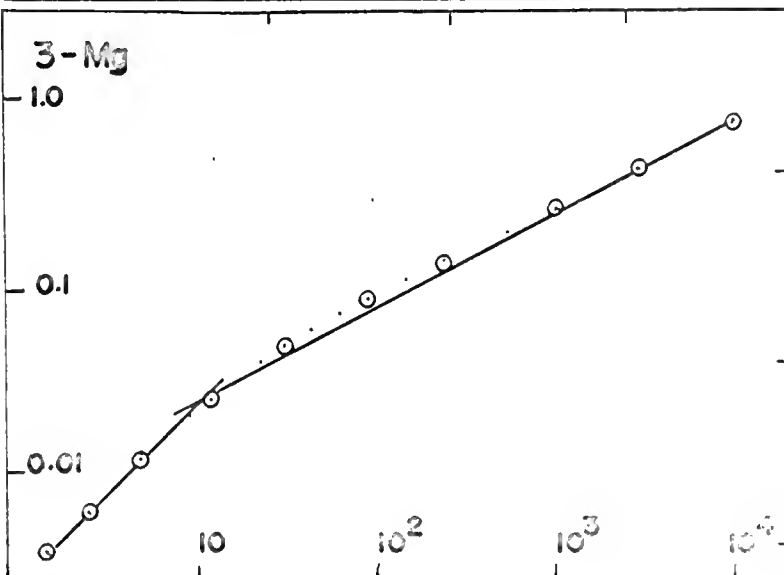
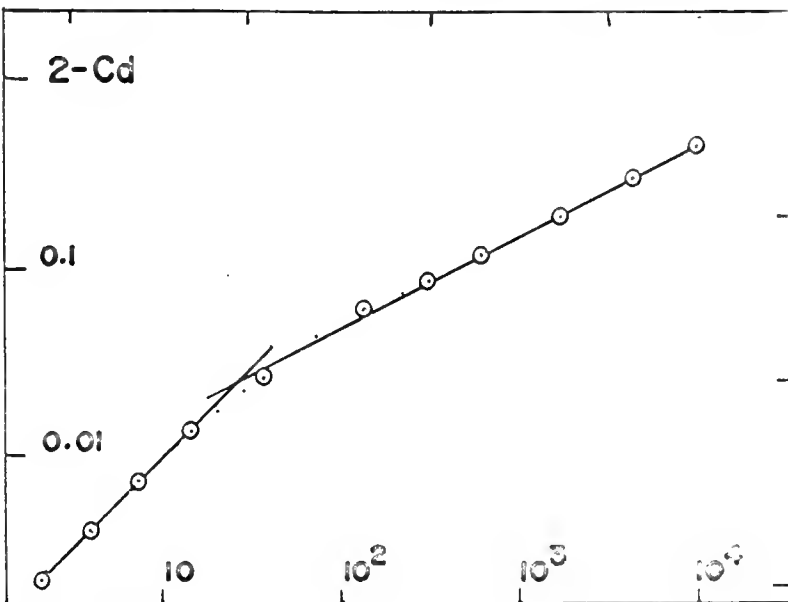
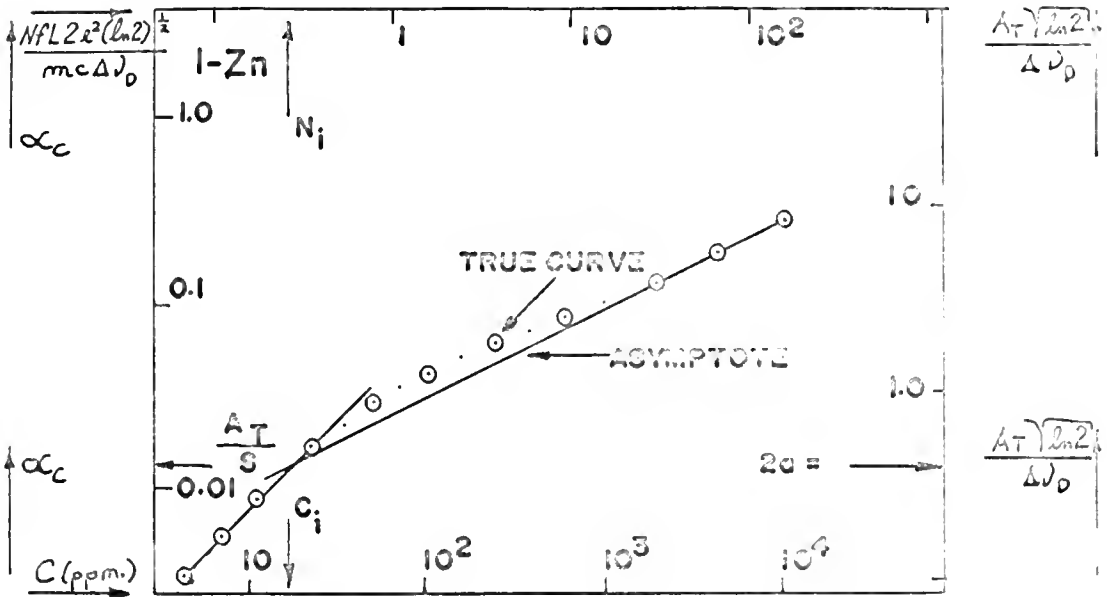


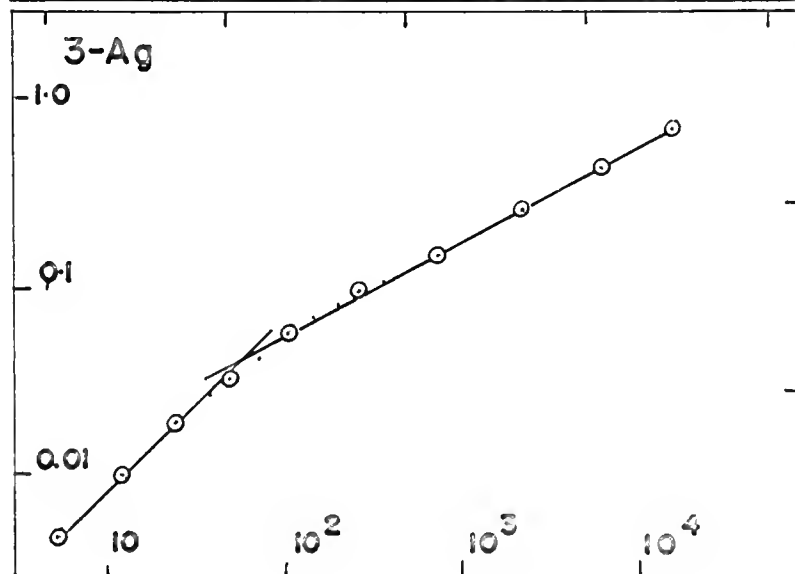
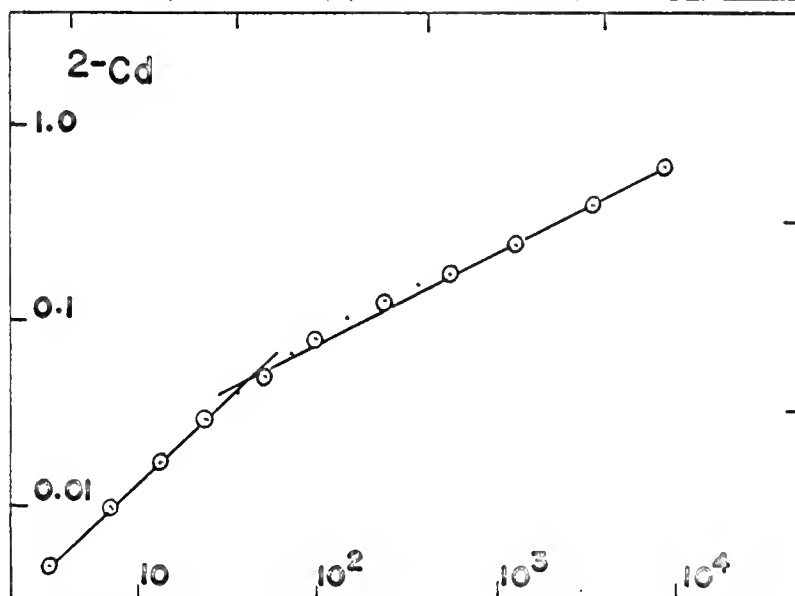
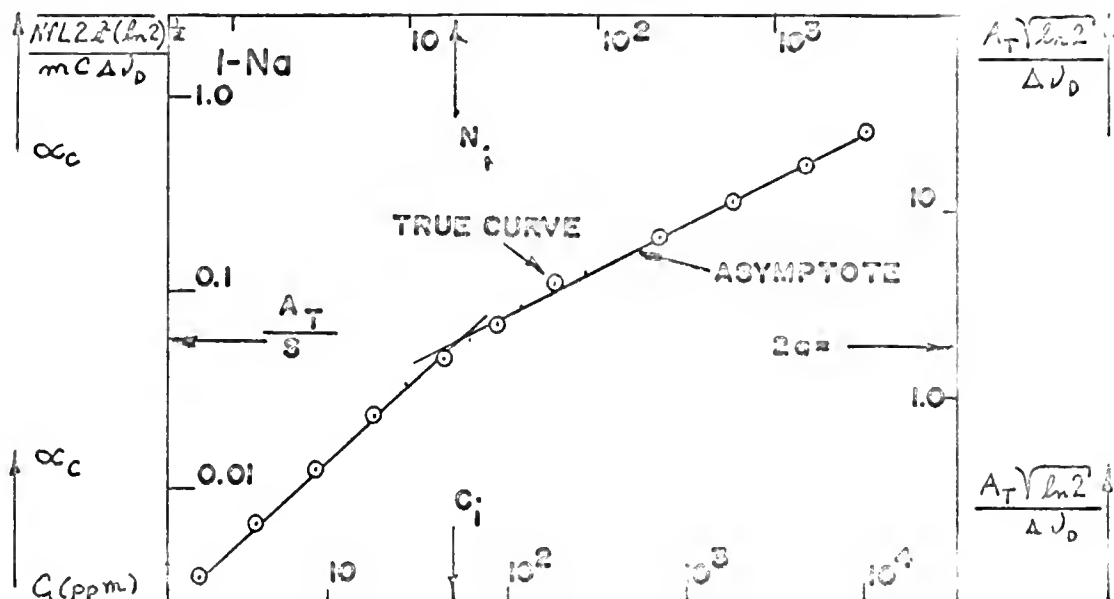
Fig. 4.-Experimental curves of growth for Ag, Cu, and Na.

(In experimental and theoretical coordinates.)

One - Sodium, 5890 Å line, in Ar/H<sub>2</sub>-E.A.

Two - Copper, 3247 Å line, in Ar/H<sub>2</sub>-E.A.

Three - Silver, 3281 Å line, in Ar/H<sub>2</sub>-E.A.



was calculated for the specified conditions. The value of the  $\underline{a}$  parameter and the location of the high density asymptote were then checked by a method described by Behmenburg and Kohn (1,2). An illustration of this checking procedure is given in Figure 5. The theoretical curves of growth used in the checking procedure were prepared from calculations given by van Trigt, Hollander, and Alkemade (38). Values of the Doppler half-intensity width and the  $\underline{a}$  parameter are given in Table 4.

From the value of the solution concentration  $C_I$ , at the intersection point, the absolute atom concentration  $N_I$ , is calculated from equation 18. It should be noted that the values of the oscillator strengths  $f$ , used in these calculations were taken from the present literature and should be considered weighted values. The  $f$  values for the alkali and alkaline earth metals used in this study are well established. The value of  $f$  for nickel, however, was calculated from the  $gf$  value given in Corliss and Bozman (5). Errors in an  $f$  value will produce direct variations in absolute atom concentration  $N_I$ ; however, in most cases in this study, variations in  $f$  are of the order of experimental error for this study. The values of  $f$  used in this study are found in Table 3. The calculated values of  $N_I$  are found in Table 4.



Fig. 5.-Illustration of test for location of high density asymptote and a parameter.

The following example illustrates the effect of an erroneous choice for the location of high density asymptote. A plot of an experimental curve of growth representing the true location of the high density asymptote and correct a parameter value of 0.25 is given. From the points U, V, and W at relatively low concentrations, one may be tempted to draw the upper density asymptote. The asymptote drawn through these points deviates only about 2 per cent from the slope of  $1/2$ , and gives an a parameter at the intersection point of the low density asymptote of 0.35. For the a parameter of 0.25, the logarithm of the total absorption at which the theoretical curve approaches the high-density asymptote equals about 0.9 and not 0.2 as is shown in the figure for erroneous construction. The value at which the logarithm of the total absorption for the theoretical curve a = 0.35, should approach the high density asymptote is about 1.2.

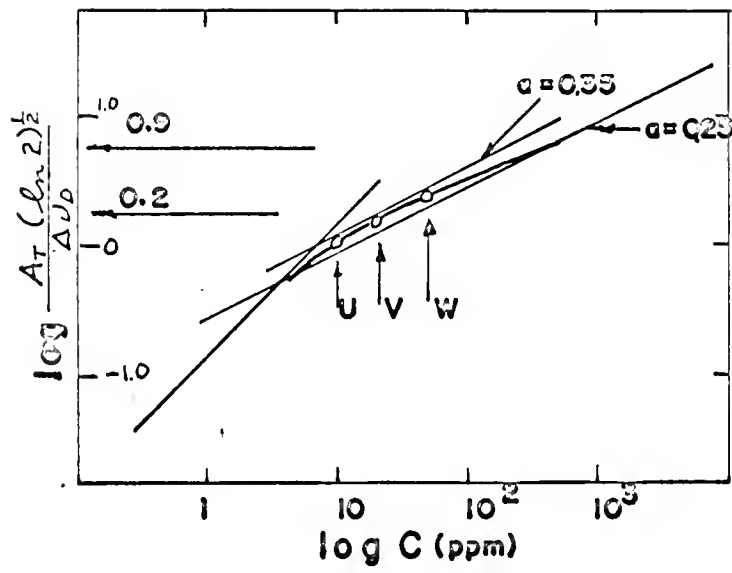


TABLE 4

VALUES OF CALCULATED SPECTRAL AND FLAME COMPOSITIONAL PARAMETERS

Element	Flame Type	$\underline{a}$	$N_I \times 10^{-11}/\text{cc.}$	$\beta_I$	$\Delta \nu_D \times 10^{-9}/\text{sec.}$	$\Delta \nu_L \times 10^{-9}/\text{sec.}$	$\Delta \nu_T \times 10^{-9}/\text{sec.}$	$\sigma_L(\text{\AA})^2$
Li	1) H <sub>2</sub> /O <sub>2</sub> ST.*	.33	1.1	.00081	6.6	2.7	7.1	29
	2) H <sub>2</sub> /O <sub>2</sub> F.R.**	.38	1.2	.0017	6.6	3.1	7.3	30
	3) Ar/H <sub>2</sub> E.A.	.22	5.5	.0022	5.6	1.5	5.8	15
	4) C <sub>2</sub> H <sub>2</sub> /O <sub>2</sub> ST.	.34	2.7	.0052	6.7	2.75	7.2	38
	5) C <sub>2</sub> H <sub>2</sub> /O <sub>2</sub> F.R.	.25	8.2	.0046	6.7	2.0	7.0	24
Na	1)	.83	1.7	.022	3.8	3.9	4.55	57
	2)	1.05	1.7	.018	3.8	4.8	6.15	63
	3)	1.00	1.7	.0031	3.3	4.0	5.2	58
	4)	1.16	4.5	.018	3.7	5.2	6.35	89
	5)	1.05	2.3	.019	4.0	5.1	6.4	88
K	1)	.75	1.1	.0060	2.3	2.1	3.05	21
	2)	.84	1.4	.0081	2.3	2.3	3.3	33
	3)	.84	0.82	.017	1.9	2.0	2.8	32
	4)	1.20	3.7	.0048	2.3	3.3	4.1	71
	5)	1.32	2.1	.0040	2.3	3.7	4.4	72
Rb	1)	.38	.30	.021	1.5	0.68	1.6	12
	2)	.75	.61	.025	1.5	1.3	2.05	21
	3)	.47	.30	.012	1.3	0.73	1.5	13
	4)	.77	.30	.016	1.5	1.4	2.1	31
	5)	.81	.68	.019	1.55	1.5	2.2	33

TABLE 4 (continued)

Element	Flame Type	$\bar{a}$	$N_I \times 10^{-11}/\text{cc.}$	$\beta_I$	$\Delta \nu_D \times 10^{-9}/\text{sec.}$	$\Delta \nu_L \times 10^{-9}/\text{sec.}$	$\Delta \nu_T \times 10^{-9}/\text{sec.}$	$\sigma_L (\text{\AA})^2$
Cu	1) H <sub>2</sub> /O <sub>2</sub> ST.	1.05	5.4	.079	4.2	5.3	6.8	95
	2) H <sub>2</sub> /O <sub>2</sub> F.R.	1.00	3.8	.075	4.2	5.0	6.6	74
	3) Ar/H <sub>2</sub> E.A.	.69	2.7	.032	3.6	3.0	4.6	52
	4) C <sub>2</sub> H <sub>2</sub> /O <sub>2</sub> ST.	.44	5.6	.033	4.25	2.3	4.8	40
	5) C <sub>2</sub> H <sub>2</sub> /O <sub>2</sub> F.R.	.56	3.1	.030	4.3	3.0	5.2	62
Ag	1)	.45	1.0	.035	3.4	1.9	3.9	33
	2)	.64	1.5	.040	3.4	2.6	4.3	40
	3)	.84	1.6	.0092	2.9	3.0	4.2	56
	4)	.96	6.0	.029	3.5	4.0	5.3	92
	5)	.95	2.5	.017	3.55	4.1	5.4	92
Mg	1)	.33	0.86	.011	7.8	4.0	8.8	60
	2)	.29	0.73	.011	7.9	2.8	8.4	37
	3)	.46	0.73	.0048	6.6	2.9	7.2	42
	4)	.41	0.21	.016	7.8	3.05	8.4	53
	5)	.32	0.82	.011	8.0	3.1	8.55	54
Ca	1)							
	2)							
	3)	.31	1.2	.00040	3.5	1.3	3.7	22
	4)	.49	.99	.00035	4.1	2.4	4.8	48
	5)	.59	.56	.00059	4.1	3.0	5.1	59
Sr	1)							
	2)							
	3)	.31	0.13	.00051	2.2	0.8	2.3	15
	4)	.66	0.86	.010	2.6	2.1	3.35	46
	5)	1.00	0.53	.00036	2.6	3.1	4.1	69

TABLE 4 (continued)

Element	Flame Type	$\bar{a}$	$N_I \times 10^{-11}/\text{cc.}$	$\beta_I$	$\Delta v_{Dx} \times 10^{-9}/\text{sec.}$	$\Delta v_{Lx} \times 10^{-9}/\text{sec.}$	$\Delta v_{Tx} \times 10^{-9}/\text{sec.}$	$\sigma_L(\text{\AA})^2$
Ni	1) H <sub>2</sub> /O <sub>2</sub> ST.							
	2) H <sub>2</sub> /O <sub>2</sub> F.R.							
	3) Ar/H <sub>2</sub> E.A.	.42	12.6	.0036	3.6	1.8	4.0	32
	4) C <sub>2</sub> H <sub>2</sub> /O <sub>2</sub> ST.	.37	42.4	.18	4.2	1.9	4.65	40
	5) C <sub>2</sub> H <sub>2</sub> /O <sub>2</sub> F.R.	.41	17.7	.011	4.2	2.1	4.7	43
Zn	1)	.30	0.54	.013	6.3	2.3	6.7	40
	2)	.19	0.35	.024	6.3	1.5	6.5	22
	3)	.44	0.61	.063	5.35	2.8	6.1	51
	4)	.21	0.94	.020	6.35	1.6	6.6	47
	5)	.28	0.41	.012	6.5	1.8	6.7	38
Cd	1)	.50	0.63	.038	4.35	2.65	5.1	47
	2)	.57	0.75	.042	4.4	3.1	5.5	47
	3)	.70	0.72	.012	3.8	3.2	5.0	61
	4)	.54	1.8	.020	4.5	2.9	5.5	67
	5)	.51	0.69	.013	4.6	2.9	5.5	64

\*ST. = Stoichiometric fuel - oxidant mixture.

\*\*F.R. = Fuel rich fuel - oxidant mixture.

The effective molecular weight  $M_a$ , of the foreign gas species producing collisional broadening represents a weighted molecular weight calculated from all gaseous species present in the flame, and was calculated from flame dissociation data given by Zaer (47). The effective molecular weight for the Ar/H<sub>2</sub>-E.A. flame was calculated assuming complete combustion of 10 per cent of the hydrogen introduced. Using these effective molecular weight values (see Table 2), values of  $\Delta\nu_L$ ,  $\Delta\nu_T$ , and  $\sigma_L$  are calculated and are found in Table 4.

## Discussion

### Discussion of errors

Before reaching any conclusions with respect to the experimental data determined in this study, a discussion of errors is necessary. However, because of the indeterminate nature of some of the errors, a detailed analysis of the total error in each case will not be given. Only an estimate of the order of magnitude of the various sources of error will be given where possible.

Errors associated with calculation of the  $\alpha$  parameter.—The relative error in measurement of the spectral band width was less than 10 per cent. A temperature variation of 100° K (a deviation of about 4 per cent) is needed to produce

a noticeable variation in the Doppler half-intensity widths. Probably the largest source of error is in drawing the asymptotes for the curve of growth to find the intersection point. Hinnov and Kohn (18,19) have commented upon this error, and concluded that the error limit for an experimentally determined  $a$  value due to the choice of the location of the asymptotes should not exceed 10 per cent. However, the high density asymptote depends heavily on the absorption values at the highest concentrations, and so this is the region of largest variation of these values. Depending on the location of the intersection point, deviations as high as 20 per cent are possible, and so the maximum relative error expected for the  $a$  parameter in this study is about 25 per cent.

Errors associated with calculation of  $N_I$  and  $\beta_I$ .—The magnitude of the error introduced in the location of the intersection point will manifest itself as a similar error in  $C_I$ . The difficulty in determining the effect of this error on  $N_I$ , lies in estimating the deviation in the effective flame path length,  $L$ . It is felt that variations as high as 50 per cent may be encountered. Similarly, the calculation of the atom formation efficiency factor  $\beta_I$ , will be expected to show relatively large deviations due to the compounding of errors from previously calculated

parameters. The relative error in estimating the aspiration efficiency  $\epsilon$ , is probably 25 per cent. Therefore,  $N_I$  and  $\beta_I$ , will have relative errors of the order of two-fold.

Errors associated with calculation of other parameters.—Random errors were reduced whenever practical by repetitive measurement. Variations in  $\Delta v_L$ , and  $\Delta v_T$  can be associated with variations expected in the a parameter. The effective collisional cross section  $\sigma_L$ , can be expected to show a somewhat larger variation than is found in the a parameter due to addition of an indeterminate error in the effective molecule weight of the perturbing gas species.

#### Comparison of results with literature data

Because of the dependence of the measured parameters upon specific flame characteristics, it is impossible to compare directly literature data to the results of this study. The experimental data determined in this study were used primarily to prepare the curves of growth by an absorption technique and to calculate the a parameter. Interpretations of other calculated data should be made with reference to the absolute magnitude of the values given. The values given in Table 5 for these parameters represent (nearly in total) those which are available in the literature.



TABLE 5  
VALUES OF SPECTRAL AND FLAME COMPOSITIONAL PARAMETERS  
TAKEN FROM LITERATURE

Element	Van Trigt, Hollander, Alkemade (38)			Kohn and Co-workers (18, 19, 20)		de Galan (9)
	<u>a</u>	$N \times 10^{-13}/\text{cc.}$	$\sigma_L(\text{\AA}^{\circ 2})$	<u>a</u>	$\sigma_L(\text{\AA}^{\circ 2})$	$\beta^e$
Li	.29 <sup>a</sup>	5.1	18	.57 <sup>c</sup>	46.5	.20
Na	.45 <sup>a</sup>	5.2	27	.79 <sup>c</sup>	59.7	.50
	.38 <sup>a</sup>	11.7	26	.79 <sup>d</sup>	65.9	
	.33 <sup>a</sup>	12.6	25			
	.41 <sup>b</sup>	10.1	30			
K	.78 <sup>a</sup>	5.3	31	1.19 <sup>c</sup>	60.4	.25
Rb				2.06 <sup>c</sup>	79.3	
Cu				.46 <sup>c</sup>	46	.97
Ag				1.03 <sup>c</sup>	83	.65
Ca	.46 <sup>a</sup>	0.85	37	.62 <sup>c</sup>	56.6	.14
	.41 <sup>a</sup>	1.1	37	.57 <sup>d</sup>	57.3	
Sr	.96 <sup>a</sup>	0.51	53	1.03 <sup>c</sup>	66.0	.13
	.85 <sup>a</sup>	0.60	53	.91 <sup>d</sup>	64.8	
Ni				.54 <sup>c</sup>	51	
Zn						.45
Cd						.49
Mg						.58

<sup>a</sup>Calculated in a CO/air flame. The different values given for some elements represents different mixtures of CO and air.

<sup>b</sup>Calculated in a C<sub>2</sub>H<sub>2</sub>/air flame.

<sup>c</sup>Calculated in a C<sub>2</sub>H<sub>2</sub>/air flame.

<sup>d</sup>Calculated in a C<sub>2</sub>H<sub>2</sub>/air - NO flame

<sup>e</sup>Calculated in a C<sub>2</sub>H<sub>2</sub>/air flame using a chamber-type burner.

When preparing curves of growth and calculating a parameters, the test developed by Behmenburg and Kohn (1, 2) is very sensitive to small deviations from the correct a parameter. Any errors in calculating  $\alpha_c$ , or in preparing the stock solutions appeared as obvious deviations from the correct slopes of the working curve (curve of growth). Perhaps the largest single source of error which produced deviations in the working curve was the spectral band width of the monochromator. Only when the slit width was increased to a relatively large width would the curve of growth show the correct slope in the high density region. This apparent failure of total absorption to be independent of spectral band width cannot be explained. Hinnov and Kohn (18,19) used large spectral band widths in their studies but offer no explanation for their use. One noticeable effect of the large spectral band width was the decrease in sensitivity in the low concentration region; this was expected, and did not affect the establishment of low density asymptote.

When a parameter values are compared, a good correlation (see Tables 4 and 5) within experimental error of this study is found for Li and K, with the data given by van Trigt, Hollander, and Alkemade (38); and for Li, Na, K, Cu, Ag, Ca, Sr, and Ni with data given by Kohn and co-workers (18,19,20) for flames of comparable composition. This is, indeed, promising for the method.

The  $\beta_I$  and  $N_I$  factors given in Table 4 and those found in Table 5 are not readily comparable because of the basic difference between the aspiration mechanism of the two types of aspirator burners used. However, the  $\beta_I$  values given in Table 4 are considerably smaller than the  $\beta$  values obtained by de Galan and Winefordner (9) (see Table 5) for the same elements in an air-acetylene flame of low burning velocity produced by a chamber type aspirator burner.

No attempt will be made to correlate  $\sigma_L$  values given in Tables 4 and 5, nor will an attempt be made to calculate values for this parameter from any of the present collisional theories (e.g., Weisskopf-Lindholm Impact Theory). The readers attention is called to the excellent articles by Behmenburg (1), and van Trigt, Hollander, and Alkemade (38) for discussion of the effects of variations in the nature of the perturbing species on the collisional cross section. The variations of the parameter found in this study from element to element and from flame type to flame type are attributed to variations in the concentration and type of perturbing species found in these flames. For this reason, these parameters are not corrected for the effects of hyperfine structure due to nuclear spin and isotopic shift and line broadening effects due to quenching collisions.

Data from this study can be used to indicate the range of variation of the a parameter, effective collisional

cross section, and total line width for conditions found in this type of flame. The  $\underline{a}$  parameter will have a value less than 1.5, an effective collisional cross section less than  $100 \text{ \AA}^2$ , and a total half-intensity line width on the order of  $10^9 \text{ sec}^{-1}$  (i.e., approximately 0.01-0.1  $\text{\AA}$  for a hypothetical line at 5000  $\text{\AA}$  wavelength). This is in line with the conclusions reached by Parsons, McCarthy, and Winefordner (32).

In conclusion, the inherent advantages of preparing working curves (curves of growth) in absorption, coupled with the predictable shape of these curves not only establishes the validity of the method, but should be of real use to the analyst. In addition, preparation of curves of growth in absorption should make this method a useful means for the study of many fundamental flame parameters.

## EXPERIMENTAL MEASUREMENTS DESIGNED TO EXTEND ANALYTICAL APPLICATIONS OF THE CONTINUOUS SOURCE

### Introduction

Atomic absorption flame spectrometry (using a line source) has enjoyed great popularity in recent years. This is primarily due to the broad applications of this technique to the trace analysis of metals. Complete commercial instruments are now available for performing absorption analyses; also a multitude of commercial components are available and these can be assembled to meet the analyst's specific needs. However, with any instrument, the analyst soon discovers limitations in his system, and these are:

(1) Choice of fuel and oxidant because of burner design.

(2) Restriction to performing only flame absorption analyses and not flame emission as well as flame absorption analyses.

(3) And most important, the time and expense involved in using line sources of radiation for nearly every element of interest.

In connection with limitation (3) above, more specific problems may be encountered with a line source, some of which are:

- (a) time involved in optically positioning the lamp for each elemental analysis;
- (b) difficulty encountered in finding lamps of satisfactory intensity, stability, and lifetime for all elements of interest to the analyst; and,
- (c) the inability to carry out simultaneous qualitative and quantitative analyses (in most cases) for more than one element.

With these limitations in mind, this investigation was carried out to develop an experimental method which would have maximum versatility without significant loss in sensitivity of measurement for performing absorption measurements.

## Experimental

### Apparatus

The instrumental set-up used to make the flame absorption measurements is shown in schematic form in Figure 6. The specific components used in the experimental set-up are given in Table 6.

As shown, the solid angle of radiation is first reduced by the housing around the xenon lamp, or by the baffle placed in front of the tungsten lamp. The radiation is chopped and passes through collimating lens  $L_1$ , where it enters the tube and is passed through it by a process involving multiple reflection (14). The resultant radiation

Fig. 6. Experimental set-up for determining limits of detection with a continuous source.

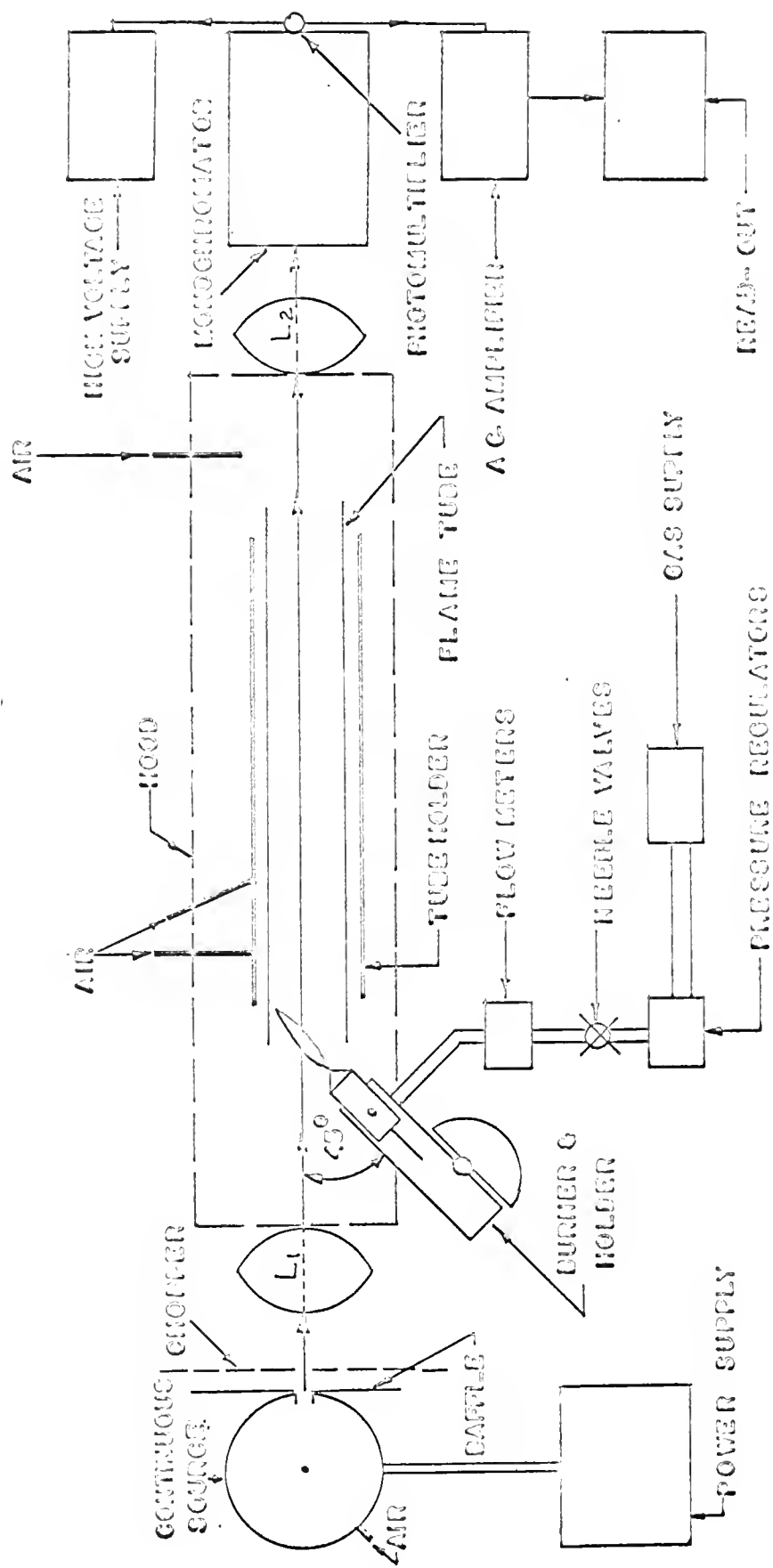




TABLE 6

EXPERIMENTAL SET-UP FOR DETERMINING LIMITS OF  
DETECTION WITH A CONTINUOUS SOURCE

1. Spectral Continua. Xenon arc, 150-watt (Englehard, Hanovia, Newark, N. J.) powered by a regulated a.c. supply (Sola Electric Co., Chicago, Ill.) used for range of 2700-6000 Å. The jacket surrounding the xenon lamp has a connector for cooling air and a baffle hole of  $5/32$ " diameter. Tungsten filament lamp (No. 2305, Beckman Instruments Inc., Fullerton, Calif.) powered by a 6 volt storage battery and used for range of 3500-8500 Å. A baffle with a  $5/32$ " hole was placed in front of the tungsten lamp.
2. Optics. Single pass, chopped at 320 cps. Chopper consists of a disc with eleven equally spaced holes rotated by an 1800 rpm synchronous motor (Bodine Electric Co., Chicago, Ill.).  $L_1$  and  $L_2$  are quartz lenses.  $L_1$  is a collimating lens, 8.0 cm. focal length. Flame tube is thick walled Vycor, 12 inches long with a 1.6 cm. O.D. and 1.0 cm. I.D. (Englehard Industries Inc., Hillside, N. J.). Tube was held in place by a laboratory clamp. The tube holder was fitted with connectors to direct air at the flame tube to prevent burnout and to extend the lifetime of the flame tube. A small hood was positioned over the flame tube and holder to remove flame gases and to cool the unit.
3. Monochromator. Jarrell-Ash, Model 82000, 0.5 meter Ebert Mount, grating spectrometer (Jarrell-Ash Co., Waltham, Mass.). Grating is ruled for 1250 lines/mm. and is blazed at 5000 Å. Reciprocal linear dispersion is 16 Å/mm. in the first order.

4. Detector-Power Supply. EMI 9558 QB photomultiplier (1650-9000 Å). Regulated d.c. power supply (No. 418 A, Fluke Mfg. Co., Seattle, Wash.).
5. Amplifier-Readout Electronics. A.C. photomultiplier output signal was fed into an O.R.N.L. Model No. 7 a.c. (23) amplifier tuned to 320 cps. The plate and filament voltages were taken from a dual power supply (No. R 100 B, Philbrick Researches, Boston, Mass.). The a.c. signal was rectified and the d.c. signal was recorded on a potentiometric recorder (Model TR, E. H. Sargent and Co., Chicago, Ill.).
6. Gas Pressure and Flow Regulation. Tank pressure is reduced by appropriate two stage high pressure regulators (The Matheson Co., Inc., East Rutherford, N. J.). The gas flow is then further regulated by a Beckman High Precision regulation unit (No. 9220, Beckman Industries Inc., Fullerton, Calif.). The resultant flow is monitored by rotameters (No. 4-15-2 Ace Glass Co., Inc., Vineland, N. J.).
7. Aspirator-Burner. Total-Consumption type. Medium bore (No. 4020, Beckman Instruments Inc., Fullerton, Calif.).

is focused by lens  $L_2$ , on the slits of the monochromator where it enters and is dispersed. The aspirator-burner and holder are mounted on a ring stand at a  $45^\circ$  angle to the optical axis of the flame tube with the tip of the burner less than one centimeter from the tube opening. The solution pipe of the aspirator burner was extended with a small piece of tubing to allow aspiration in a horizontal position.

The flow rate of aspirating gas was 2.25 l./min. for argon and 2.75 l./min. for air. The resultant solution flow rate was then 1.0 ml./min. The flow rate of hydrogen was optimized for each element and is given in Table 7.

The slit width used throughout this investigation was 10 microns. This corresponds to a theoretical spectral band width of  $0.16 \text{ \AA}$  in the first order. The spectral band width, however, was measured by the method described in the previous section, and was found to be  $0.32 \text{ \AA}$ .

Near the limit of detectability, a scale expansion technique was used to increase the accuracy of measurement. Scale expansion was accomplished by proper adjustment of the zero suppress and by using a lower scale setting (i.e., 12.5 mV. to 4.0, 2.5, or 1.25 mV.) on the recorder. The phototube voltage used during the determination of each element is given in Table 7.

TABLE 7

EXPERIMENTAL CONDITIONS AND LIMITS OF DETECTION OBTAINED FOR 21 ELEMENTS USING THE CONTINUOUS SOURCE

Element	Wavelength (A)	H <sub>2</sub> Flow Rate (liters/min.)	Phototube Voltage (Volts)	Limits of Detectability (p.p.m.)		
				Continuous Source		Line Source
				This Work	Fassel, et al. (12)	Slavin (35)
1. Li <sup>b</sup>	6707	4.5 <sup>f</sup>	1360	0.01	0.004	0.005
2. Na <sup>a</sup>	5890	4.0 <sup>f</sup>	1300	0.02	0.03	0.005
3. K <sup>a</sup>	7665	4.5 <sup>f</sup>	1500	0.07	0.03	0.005
4. Rb <sup>a</sup>	7800	5.3 <sup>f</sup>	1500	0.01	0.04	0.02
5. Ag <sup>a</sup>	3281	4.2	1060	0.01	0.2	0.02
6. Mg <sup>a</sup>	2852	5.6	1300	0.007	0.01	0.003
7. Ca <sup>b</sup>	4227	7.5	970	0.09	0.03	0.01
8. Sr <sup>b</sup>	4607	11.5	1020	0.02	0.06	0.02
9. Ba <sup>b</sup>	5535	13.0	1000	0.1	0.9	1.0
10. Cu <sup>a</sup>	3247	13.0	1140	0.02	0.05	0.005
11. Mn <sup>e</sup>	2798	8.5	1100	0.01	0.07	0.01
	4032	8.5	1100	0.5	--	--
12. Ni <sup>c</sup>	3414	6.2	1140	0.5	0.7	0.05
	4032	6.2	1140	0.1	--	--
13. Cr <sup>d</sup>	3579	7.7	1130	0.2	0.2	0.01
14. Co <sup>b</sup>	3526	4.8	1100	0.4	3	0.15
15. Fe <sup>c</sup>	3021	4.8	1200	0.04	1	0.05
16. Bi <sup>c</sup>	3067	4.5	1000	0.07	4	0.2
17. Sn <sup>c</sup>	2863	4.6	1140	0.02	6	2.0
18. Pb <sup>b</sup>	2833	4.6	1100	0.2	2	0.15

TABLE 7 (continued)

Element	Wavelength (Å)	H <sub>2</sub> Flow Rate (liters/min.)	Phototube Voltage (Volts)	Limits of Detectability (p.p.m.)		
				This Work	Continuous Source Fassel, et al. (12)	Line Source Slavin (35)
19. Ga <sup>c</sup>	2874	8.4	1100	0.5	2	1.0
20. In <sup>b</sup>	3040	5.8	1170	0.04	0.2	0.5
21. Tl <sup>c</sup>	3775	4.6	1100	0.02	0.6	0.2

<sup>a</sup>These elements were prepared using their chloride salts.

<sup>b</sup>These elements were prepared using their nitrate salts.

<sup>c</sup>These elements were prepared by dissolving the pure metal in a minimum amount of concentrated HCl.

<sup>d</sup>These elements were prepared from dichromate salt.

<sup>e</sup>These elements were prepared by dissolving MnO<sub>2</sub> in HCl.

<sup>f</sup>Limits of detectability using air/H<sub>2</sub> flame.

## Solutions

Stock solutions of 1000 ppm for each element were prepared by dissolving the appropriate salt in aqueous, or the metal in acidified-aqueous solution. More dilute solutions were made by successive dilution of this stock solution. In the case of the solutions prepared by dissolving the metal in acid, a small but constant concentration of acid was maintained in each dilution. The specific salts used to prepare the stock solutions are given in Table 7.

## Procedure

The wavelength used for the atomic absorption measurements of each element is selected by aspirating a 50 ppm solution of the element of interest and then manually scanning to locate the wavelength of maximum absorption. Scanning the wavelength range is useful for the following reasons:

(1) The optimum wavelength for analysis can be determined if more than one wavelength is available (e.g., the transition metals).

(2) The noise on the background signal adjacent to the wavelength of interest can be measured.

(3) The presence of contaminating elements in solution which may interfere with the element under investigation can be determined.

The flame tube is flushed after each measurement by continuously aspirating water. This is necessary to extend the lifetime of the flame tube by preventing burn out and salt fusion, and to reduce the noise on the background signal. Periodic flushing (between use in analysis) of the tube with dilute  $\text{HNO}_3$  minimizes the decrease in reflectivity of the flame tube due to salt fusion.

Additional discussion of the experimental technique and problems encountered when using the flame tube may be found in articles by Fuwa and Vallee (14), and Koirtyohann and Feldman (24).

## Results

Limits of detectability for twenty-one elements measured using the experimental technique described above are given in Table 7. The limit of detectability (45) is defined as that solution concentration resulting in a signal-to-noise ratio of 2.0. Noise is defined as peak-to-peak divided by 2. The limits of detectability given in Table 7 represent an average of nine determinations having about a 50 per cent relative standard deviation. It should be noted that the values given in Table 7 represent the lowest obtainable using the experimental set-up described in the apparatus section of this chapter, and various combinations of fuel and oxidant. In each case for each

element, various combinations of  $C_2H_2$ ,  $H_2$ ,  $O_2$ , and air as well as argon were tested to see which combination gave the lowest limits of detectability.

Relative standard deviations were calculated on the basis of nine runs for 100 ppm and at a ten-fold concentration higher than that determined for the limit of detectability as well as at the limit of detectability. For concentrations ten-fold higher than the limit of detectability, the relative standard deviation was never larger than 1.0 per cent for all elements run; whereas at 100 ppm, the relative standard deviation was between 2.0 and 8.5 per cent, depending on the particular element. In Figure 7, typical working curves for three elements are given. The data for these three elements are treated in the conventional manner (i.e., plots of absorbance vs. concentration) to illustrate the similarities between the two types of absorbance working curves (i.e., curves plotting relative absorption and absorbance vs. concentration). As discussed in a previous section (see Figure 4 for fraction of intensity vs. concentration working curves for the same three elements), the shapes of the working curves are characterized by a linear portion in the low concentration range which extends to about a 10 per cent absorption. From Figure 7 for the flame tube study, it can be seen that the working curve for silver is linear from 0.01 ppm to about 100 ppm, whereas the copper



and sodium curves are linear from about 0.02 to about 30 ppm. All other elements give curves similar to those of sodium and copper.

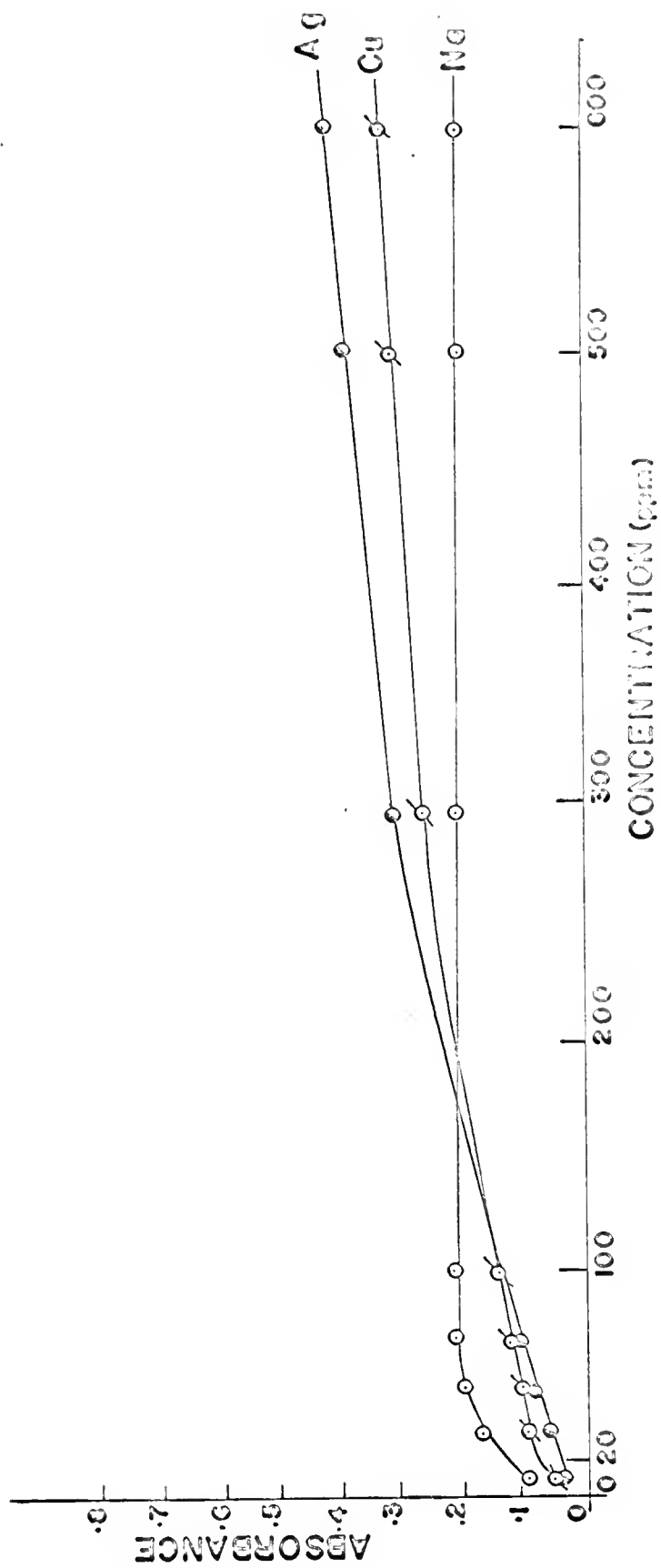
Due to the extreme curvature of the working curves at high concentrations, a working curve must be prepared prior to performing quantitative measurements. Fassel and co-workers (12) have described the signal corrections which must be considered when preparing absorbance versus solution concentration working curves. From a comparison of the two types of working curves (see Figures 4 and 7), it should be noted that when it is necessary to work with high solution concentrations falling on the nonlinear portion of the absorbance curve, the experimental procedure described in the Introduction would be preferred because of the more favorable slope (proportional to concentration) in this region.

### Discussion

To meet the requirements imposed upon the experimental system, all components chosen for the analysis system are characterized by a wide range of operating conditions in order to meet the varying needs of the analyst.

A spectral continuum as a source of radiation certainly eliminates many of the restrictions placed on atomic absorption by the use of line sources of radiation.

Fig. 7. Analytical absorbance curves for Ag, Cu, and Na obtained using a continuous source.



The added versatility of the qualitative aspect of atomic absorption analyses eliminates this present inherent limitation of the line source. In this study, a qualitative investigation and quantitative estimate of the sensitivity of the major atomic absorption lines of each element was used to determine the absorption lines for measurement.

The total-consumption aspirator-burner was chosen primarily because of the simplicity of sample introduction, and because of the wide range of fuels and oxidants which can be used with it. However, one major disadvantage of the total-consumption aspirator-burner for atomic absorption studies is the very short absorption path length of the flame even under very fuel-rich conditions. This is a serious handicap when sensitivity is desired. Several attempts were made at finding a means for lengthening the path length of the radiation through this flame. Multiple pass of radiation from mirrors through the flame, multiple burners (in line), and multiple pass of radiation through multiple burners were just a few of the designs tried. However, it was found that the flame tube, when combined with the argon/hydrogen-entrained air flame ( $\text{Ar}/\text{H}_2\text{-E.A.}$ ) gave results superior to all other designs. The flame tube not only extends the path length of the radiation through the flame, but in addition, because of its cage effect (it directs the flame in the radiation path and prevents outer

diffusion of atoms), it extends the residence time of atoms in the light path.

Fuwa and Vallee (14) were the first to suggest the use of the flame tube for atomic absorption analyses; however, they used line sources of radiation. Later Koirtyohann and Feldman (24), and more recently, Koirtyohann and Pickett (25,26,27) have determined limits of detectability and discussed possible sources of spectral interferences using the flame tube. It is interesting to note that although their application involved use of a line source of radiation, a spectral continuum source was suggested as a means of correcting for spectral interferences.

The flame tube has the additional advantage that misalignment of the aspirator-burner or incorrect positioning of the flame in the light path is not as critical as alignment of the line source and acetylene-air flame used with most chamber type aspirator-burners. Of course, alignment of the flame tube in the light path is critical.

The Ar/H<sub>2</sub>-E.A. flame was used in these studies because of the success of this flame in atomic fluorescence (39) and atomic emission (46) studies. The total-consumption aspirator-burner combined with the Ar/H<sub>2</sub>-E.A. flame is an efficient method of producing atoms. This is evident from data given in Table 7.

The good sensitivity of the Ar/H<sub>2</sub>-E.A. flame is a result of two factors, namely: the Ar/H<sub>2</sub>-E.A. flame has a very low background which results in greater sensitivity (39,45); and the total-consumption aspirator-burner in conjunction with the Ar/H<sub>2</sub>-E.A. flame and the flame tube results in greater efficiency of atomization than is obtained for most other aspirator-burner-flame systems. The longer residence time of atoms in the flame tube and the reducing characteristics of the flame gases decrease compound formation, and, therefore, increase efficiency of atomization.

The requirements of the monochromator when using a spectral continuum of radiation are, of course, more critical than when using a line source of radiation. For the case where the line source is used, Walsh (41) concluded that because the decrease in the peak intensity of the line was measured, only a low resolution monochromator capable of isolating the spectral line from the source was required. For the case where the spectral continuum is used, Winefordner (42) has shown that as the spectral band width of the monochromator approaches the absorption line width of the atoms in the flame, the sensitivity of measurement will increase almost linearly with decrease in the spectral band width. This effect undoubtedly accounts in part for the increase in sensitivity found for elements in this study. These results confirm the statement by Gibson, Grossman, and Cooke

(16) that a medium resolution, large aperture bench-sized monochromator combined with a scale expansion technique should give good sensitivity; the monochromator used in their study and in this one were identical.

One additional comment about the monochromator. If the analyst wishes to analyze for elements which have widely varying resonance wavelengths (e.g., cesium at 8500 Å and zinc at 2100 Å), some of the difficulties encountered with the transmission range of the monochromator can be overcome by choosing a grating with a long wavelength blaze (e.g., 7500 Å in first order). In the lower wavelength region where intensity in the first order is low (for a 7500 Å blazed grating), higher orders of the radiation can be used satisfactorily.

In conclusion, using the experimental system previously described, the limits of detectability are comparable to or greater than the best values listed in the literature for a line source, acetylene-air, chamber-type flame system and the values listed by Fassel and co-workers (12) for the continuous source, fuel-rich acetylene-oxygen, total-consumption system (see Table 7). This certainly indicates that the spectral continuum (in conjunction with the flame tube and the Ar/H<sub>2</sub>-E.A. flame system) as a source of excitation should be competitive to the use of the line source and a typical air-acetylene flame and chamber-type aspirator-

burner measurements in addition to providing added versatility to the system, which the analyst can always use.



## FUTURE WORK

The work presented in this dissertation demonstrates the feasibility of using a continuous source in atomic absorption flame analyses. However, during this investigation, other areas for research became apparent, primarily as a result of the interpretation of data concerning the measured a parameters. Research is definitely needed to:

(1) Establish the reasons for the wide divergence in atom formation efficiency factors found for chamber and total consumption-type burners; an approach utilizing the measurement of absolute emission intensity and total absorption for elements atomized in both types of burners could be used to determine the absolute atom concentration.

(2) Establish the relationship between the spectral band width required to produce a satisfactory curve of growth and the half-intensity width of the line under investigation; as the first step, an instrument of high resolving power (interferometer) could be used to establish the profiles of the lines produced in this type of flame (see Appendix I).

(3) Determine the nature of the perturbing species in the flame produced from a total consumption-type burner; the effect of the large quantity of water introduced into this flame should be established.

The absorption technique used in this study should be used to determine fundamental atom parameters (such as those investigated in this study) in flames of low burning velocity from a chamber-type burner. These values will be compared with those previously determined by one of the emission techniques.

## CONCLUSIONS

The major contributions made in this dissertation are:

- (1) Application of theoretical relationships derived in astrophysics to atomic absorption measurements with a continuous source.
- (2) Derivation of a relationship between fraction of radiation absorbed  $\alpha$ , and absorber concentration and usefulness of this relationship for preparation of experimental working curves over wide ranges of absorber concentration (working curves are useful over a wide concentration range and any interferences can be readily detected by a change in the characteristic shape of such a working curve).
- (3) Measurement of spectral parameters such as damping constants and collisional cross-sections of lines of atoms in flames of high burning velocity.
- (4) Demonstration of the usefulness of the continuous source and a  $\text{Ar/H}_2$ -E.A. flame in a quartz tube for the detection of low concentrations of a number of elements by atomic absorption flame spectrometry.

The advantages of using a continuous source and a  $\text{Ar/H}_2$ -E.A. flame are:

(1) The low limits of detection obtained are comparable with similar values obtained using line sources.

(2) The use of one experimental system for the qualitative and quantitative determination of a large number of elements in a variety of sample matrices.

The only serious disadvantage of such a system is that an intense continuum and a medium resolution rather than a low resolution monochromator must be used. However, such a system is still considerably cheaper and more versatile than an atomic absorption spectrometer using line sources.

## APPENDIX I

If the spectral band width,  $s$ , is of the same order of magnitude as the absorption line half-intensity width of atoms in the flame gases, for example, as for alkali atoms at high atom concentrations in flames, then the measured value of  $\alpha_c$ , will not be the same as  $A_T/s$  as defined by equation 12. A correction factor relating the measured  $\alpha_c$  to  $A_T/s$  can be determined by assuming a certain slit function distribution, for example, if a triangular slit function  $g_\lambda$ , is assumed then

$$\alpha_c = \frac{\int_0^\infty g_\lambda (1 - e^{-k_\lambda L}) d\lambda}{s}, \quad (23)$$

and if the above expression is evaluated, then

$$A_T \approx \frac{\alpha_c}{s} \left( 1 + \frac{\alpha_c}{3} \right), \quad (24)$$

where the term in parenthesis is a correction factor to convert the measured value of  $\alpha_c$  to the defined value of  $\alpha_c$  (equation 12). As can be noted for the above case, little error results as long as the measured values of  $\alpha_c$  are less than 0.1. However, for the alkali metals,  $\alpha_c$  is greater than 0.1 unless slit widths greater than 200 microns are used.

# LITERATURE CITED

1. Behmenburg, W., J.O.S.R.T. 4, 177 (1964).
2. Behmenburg, W., Kohn, H., J.O.S.R.T. 4, 165 (1964).
3. Bockris, J. O'M., White, J. L., MacKenzie, J. D., "Physiochemical Measurements at High Temperatures," Butterworths, London, 1959.
4. Broida, H. P., Lalos, G. T., J. Chem. Phys. 20, 1466 (1952).
5. Corliss, C. H., Bozman, W. R., "Experimental Transition Probabilities for Spectral Lines of Seventy Elements," N.B.S. Monograph No. 53, Washington, D.C., 1962.
6. Crosswhite, H. M., "The Spectrum of Iron I," John Hopkins Spectroscopic Rept. No. 13, August, 1958.
7. de Galan, L., Personal Communication.
8. de Galan, L., Winefordner, J. D., Anal. Chem., in press, 1966.
9. de Galan, L., Winefordner, J. D., Submitted 1966.
10. de Vos, J. C., Physica 20, 690 (1954).
11. Fassel, V. A., Mossotti, V. G., Anal. Chem. 35, 252 (1963).
12. Fassel, V. A., Mossotti, V. G., Grossman, W. E. L., Kniseley, R. A., Spectrochim. Acta. 22, 347 (1966).
13. Fery, Ch., Comptes Rendus 137, 909 (1903).
14. Fuwa, K., Vallee, B. L., Anal. Chem. 35, 942 (1963).
15. Gaydon, A. G., Wolfhard, H. G., "Flames, Their Structure, Radiation and Temperature," Chapman and Hall Ltd., London, 1960.

16. Gibson, J. H., Grossman, W. E. L., Cooke, W. D., "Analytical Chemistry" (proc. Feigl Anniv Sym.) pg. 296, Elsevier, 1962.
17. Hermann, R., Alkemade, C. Th. J., "Chemical Analysis by Flame Photometry" (translated by P. T. Gilbert), John Wiley and Sons, New York, 1963.
18. Hinnov, E., J. Opt. Soc. Am. 47, 151 (1957).
19. Hinnov, E., Kohn, H., J. Opt. Soc. Am. 47, 156 (1957).
20. Hoffman, F. W., Kohn, J., J. Opt. Soc. Am. 51, 512 (1961).
21. Hollander, Tj., Thesis, Utrecht (1964).
22. Ivanov, N. P., Kozireva, N. A., Zh. Analit. Kim. 19, 1178 (1964).
23. Jones, H. C., Fisher, J. D., Kelley, M. T., "Fifth Conference on Analytical Chemistry in Nuclear Reactor Technology," Gatlinburg, Tennessee, October, 1961. T.I.D. 7629.
24. Koirtzyohann, S. R., Feldman, C., "Developments in Applied Spectroscopy," Vol. 3, J. E. Forrester ed. Plenum Press, New York, 1964.
25. Koirtzyohann, S. R., Pickett, E. E., Anal. Chem. 37, 601 (1965).
26. Koirtzyohann, S. R., Pickett, E. E., Anal. Chem. 38, 585 (1966).
27. Koirtzyohann, S. R., Pickett, E. E., Anal. Chem. 38, 1087 (1966).
28. Ladenburg, R., Reiche, F., Ann. d. Phys. 42, 181 (1913).
29. Minkowski, R., Z. f. Phys. 36, 839 (1926).
30. Mitchell, A. C. G., Zemanski, M. W., "Resonance Radiation and Excited Atoms," Cambridge University Press, London, 1961.
31. Parsons, M. L., Winefordner, J. D., Appl. Spect. in press, 1966.
32. Parsons, M. L., McCarthy, W. J., Winefordner, J. D., Anal. Chem. in press, 1966.

33. Penner, S. S., "Quantitative Molecular Spectroscopy and Gas Emissivities," Addison-Wesley, Reading, Mass., 1959.
34. Rubeska, I., Svoboda, V., Anal. Chim. Acta 32, 253 (1965).
35. Slavin, W., Atomic Absorption Newsletter, No. 24, Sept., 1964.
36. Unsöld, A., "Physic der Sternatmosphären," Springer, Berlin, 1955.
37. van der Held, E. F. M., Ornstein, S., Z. f. Phys. 77, 459 (1932).
38. van Trigt, C., Hollander, Tj., Alkemade, C. Th. J., J.Q.S.R.T. 5, 813 (1965).
39. Veillon, C., Mansfield, J. M., Parsons, M. L., Winefordner, J. D., Anal. Chem. 38, 204 (1966).
40. Vickers, T. J., Remington, L. D., Winefordner, J. D., Anal. Chim. Acta in press, 1966.
41. Walsh, A., Spectrochim. Acta. 7, 108 (1955).
42. Winefordner, J. D., Appl. Spect. 17, 109 (1963).
43. Winefordner, J. D., Mansfield, C. T., Vickers, T. J., Anal. Chem. 35, 67 (1963).
44. Winefordner, J. D., Vickers, T. J., Anal. Chem. 36, 1939 (1964).
45. Winefordner, J. D., Vickers, T., Anal. Chem. 36, 1947 (1964).
46. Zacha, K., Winefordner, J. D., Anal. Chem. in press, 1966.
47. Zaer, R. A., Thesis, Paris (1935).




## BIOGRAPHICAL SKETCH

William Walter McGee III was born June 27, 1939, in Toledo, Ohio. In June, 1957, he was graduated from Jesup W. Scott High School, Toledo, Ohio. In June, 1961, he received the degree of Bachelor of Science from the University of Toledo, Toledo, Ohio. In June, 1962, he received the degree of Master of Science from the University of Toledo, Toledo, Ohio. From September, 1963, until the present time, he has pursued his studies toward the degree of Doctor of Philosophy.

He is married to the former Mary Ann Nietz of Toledo, Ohio.

This dissertation was prepared under the direction of the chairman of the candidate's supervisory committee and has been approved by all members of that committee. It was submitted to the Dean of the College of Arts and Sciences and to the Graduate Council, and was approved as partial fulfillment of the requirements for the degree of Doctor of Philosophy.

December 17, 1966

  
\_\_\_\_\_  
Dean, College of Arts and Sciences

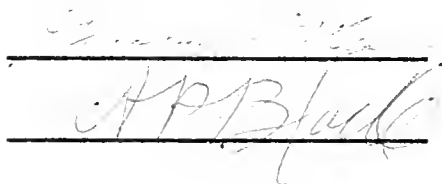
\_\_\_\_\_  
Dean, Graduate School

Supervisory Committee:

\_\_\_\_\_  
Chairman

  
\_\_\_\_\_

\_\_\_\_\_

  
\_\_\_\_\_



